Detrital zircon ages from the Lower Santa Rosa Formation, Chiapas: implications on regional Paleozoic stratigraphy

Bodo Weber[1,*], Victor A. Valencia[2], Peter Schaaf[3], and Fernando Ortega-Gutiérrez[4]

[1] División Ciencias de la Tierra, Centro de Investigación Científica y de Educación Superior de Ensenada (CICESE), Carretera Tijuana-Ensenada Km. 107, 22860 Ensenada, B.C., Mexico.
[2] Department of Geosciences, University of Arizona, 1040 East Fourth St, Tucson AZ, 85721-0077 USA.
[3] Instituto de Geofísica, Universidad Nacional Autónoma de México (UNAM), Ciudad Universitaria, Del. Coyoacán 04510 Mexico, D.F., Mexico.
[4] Instituto de Geología, Universidad Nacional Autónoma de México (UNAM), Ciudad Universitaria, Del. Coyoacán 04510 Mexico, D.F., Mexico.
** bweber@cicese.mx*

ABSTRACT

Samples from the Rio Aguacate sequence that defines the Lower Santa Rosa Formation (SRF) in Chiapas were collected in the Jaltenango river valley that is currently partly flooded by the La Angostura Lake. U-Pb geochronologic analyses by Laser-Ablation Multicollector ICPMS have been conducted on 209 zircons from two quartz-rich samples of a monotonous slate and phyllite section cropping out above the lake. The maximum depositional age of the upper sample is defined by an overlapping group of three zircons having ages from 325 to 315 Ma. The youngest cluster of ages from the the second sample, which comes from an outcrop ~3000 meters below the first, range from 341 to 331 Ma. The results indicate that most of the Santa Rosa Formation (SRF) accumulated in Mississippian time. Most detrital zircons have ages that correspond to the Pan-African-Brasiliano orogenic cycle (~700–500 Ma). Secondary peaks in the age spectra are Mesoproterozoic (~1600–900 Ma), Paleoproterozoic (~2150 Ma), Archaean (~2.6–3.3 Ga), and also Silurian-Lower Devonian (~420–360 Ma). Mesoproterozoic zircons with a major peak at 1237 Ma and a second at 1025 Ma are present only in the stratigraphically lower sample. Otherwise, the provenance ages of the Lower SRF are similar to those from the Upper SRF, indicating that the SRF probably comprises a continuous sequence. The results further indicate that early Paleozoic sedimentary rocks of the Maya block are not part of the SRF . Similarities in detrital age distributions suggest a potential correlation with the Cosoltepec Formation of the Acatlán Complex, but a correlation with Paleozoic strata (Ixtaltepec and Santiago Formations) covering the Oaxacan complex is not indicated.

Key words: provenance age, zircon, Santa Rosa Formation, Paleozoic, SE Mexico.

RESUMEN

Muestras de la secuencia "Río Aguacate", la cual fue definida como la Formación Santa Rosa Inferior en el estado de Chiapas, fueron recolectadas en el valle del Río Jaltenango que actualmente se encuentra parcialmente cubierto por la presa de La Angostura. Se llevaron a cabo análisis geocronológicos de 209 zircones con el método de U-Pb con ablación láser en un ICPMS multicolector. Los zircones fueron separados de dos muestras ricas en cuarzo tomadas de la secuencia monótona de pizarras y filitas que destaca del agua. La edad máxima de sedimentación de la muestra superior está definida por un grupo de tres zircones que arrojan edades entre 325 y 315 Ma. El grupo de zircones con edades más jóvenes de la segunda muestra, que se tomó de un afloramiento que se encuentra ~3000 m debajo de la muestra

anterior, varía entre 341 y 331 Ma. Los resultados indican que la mayor parte de la Formación Santa Rosa SRF fue acumulada durante el Misisipiano. La mayoría de los zircones detríticos tienen edades que corresponden al ciclo orogénico del Pan-Africano-Brasiliano (~700–500 Ma). Picos secundarios en los espectros de edades son del Mesoproterozoico (~1600–900 Ma), Paleoproterozoico (~2150 Ma), Arqueano (~2.6–3.3 Ga) y también del Silúrico-Devónico Inferior (~420–360 Ma). Zircones mesoproterozoicos, con un pico mayor en 1237 Ma y uno secundario en 1025 Ma, se encuentran solamente en la muestra estratigráficamente inferior. Las edades de proveniencia de la Fm. Santa Rosa Inferior son similares a las de la Fm. Santa Rosa Superior, indicando que la Formación Santa Rosa es probablemente una secuencia continua. Además, los resultados indican que los sedimentos del Paleozoico temprano del bloque Maya no forman parte de la SRF. Similitudes en las distribuciones de edades entre la Formación Santa Rosa y la Formación Cosoltepec del Complejo Acatlán señalan una posible correlación entre ambas, mientras que una correlación con sedimentos Paleozoicos (Formaciones Ixtaltepec y Santiago) que cubren el Complejo Oaxaqueño no está indicada.

Palabras clave: edad de proveniencia, zircón, Formación Santa Rosa, Paleozoico, SE de México.

INTRODUCTION

The southern edge of the Maya block (Dengo *et al.*, 1985) in southeastern Mexico and Guatemala (Figure 1) is truncated by a set of Cenozoic faults that form the complex boundary between the North American plate and the Caribbean plate (Chortis block) in Central America (*e.g.*, Anderson and Schmidt, 1983; Burkart and Self, 1985; Burkart *et al.*, 1987). The geologic relationships along the Maya-Chortis boundary are characterized by fault-bounded stratigraphic packages which differ in metamorphic grade and deformation style. Five individual crustal slices were recently identified as independent tectostratigraphic terranes or blocks between the Maya and the Chortis blocks (Ortega-Gutiérrez *et al.*, 2007). Therefore, the stratigraphy of the sedimentary units of every individual block can help to understand the significance of possible correlations between each other and the adjacent major continental blocks. In order to form a basis for such correlations, the stratigraphic successions in the Maya and the Chortis blocks, on either side of the plate boundary, must be thoroughly known. For such a purpose, the statistical analysis of U-Pb ages of detrital zircons is a powerful tool (*e.g.*, Fedo *et al.*, 2003), even when the rocks underwent metamorphic overprint or deformation.

In this contribution we enhance the Paleozoic stratigraphy of the Maya block with detrital zircon ages from recently recovered outcrops of the Lower Santa Rosa

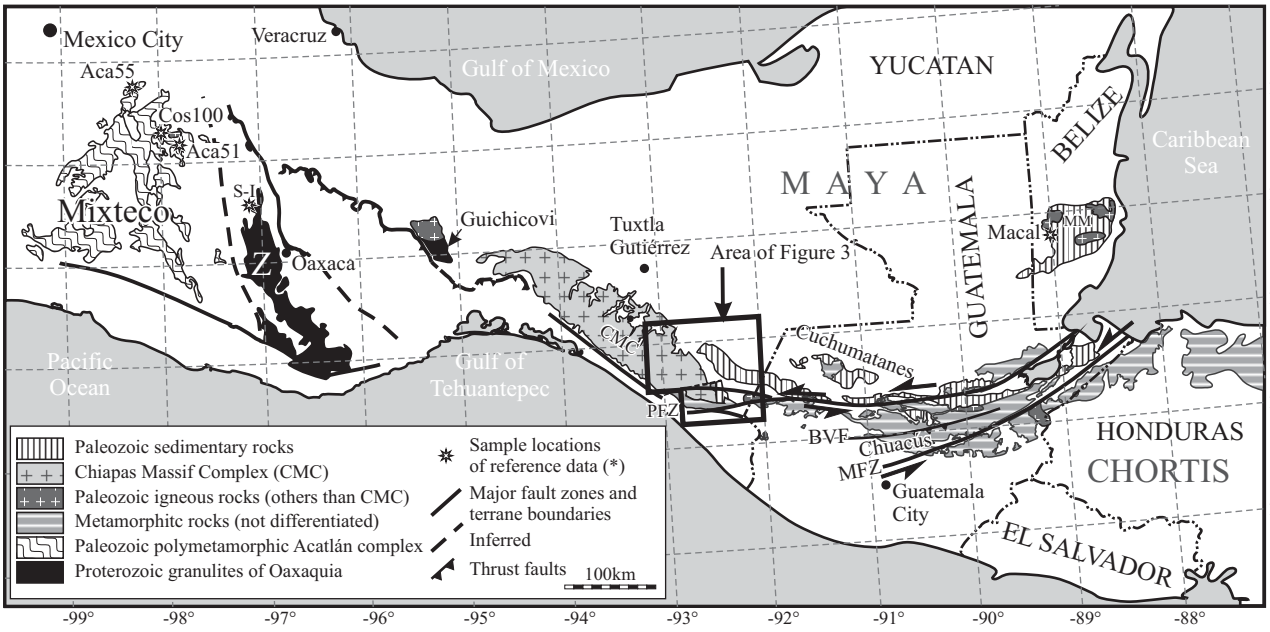

Figure 1. Geologic map showing pre-Mesozoic rocks exposed in southern México and Central America (modified after Ortega-Gutiérrez *et al.*, 1992, 2007, and French and Schenk, 1997). Abbreviations: BVZ: Baja Verapaz fault, CMC: Chiapas Massif Complex, MFZ: Motagua fault zone, MM: Maya Mountains, PFZ: Polochic fault zone, Z: Zapoteco terrane. (*: Aca51 and Aca55 from Talavera-Mendoza *et al.*, 2005; Cos100 from Keppie *et al.*, 2006, S-I, Santiago and Ixtaltepec formations, from Gillis *et al.*, 2005; Macal from Martens *et al.*, submitted).

Formation (SRF) in Chiapas. We present U-Pb isotope data of 209 individual zircon grains from two samples from the type locality of this Paleozoic sequence where it was originally described by Hernández-García in 1973. With these data, together with complementary detrital zircon ages published for the Upper SRF (Weber *et al.*, 2006), we will be able to improve the stratigraphy of the Maya block, which in turn will help in the endeavor to correlate the Maya with the adjacent crustal blocks. The results are of importance for both provenance of the sediments and their stratigraphic age. This is the first study of the revisited Lower SRF in Chiapas since its discovery and stratigraphic subdivision by Hernández-García (1973). Although this issue is focused on the Mesozoic and Cenozoic evolution of southern Mexico and the Chortis block, in this paper we provide information on older, pre-Mesozoic rocks. However, we feel confident that this contribution might be of avail to associate subsequently disrupted units within the Maya-Chortis border zone.

GEOLOGIC OVERVIEW

The Maya block is the southeasternmost of the Mexican terranes (Figure 1). It includes the Cretaceous carbonate platform of the Yucatan peninsula and extends across northern Guatemala and southeastern México to the Tehuantepec isthmus (Dengo *et al.*, 1985). Pre-Mesozoic rocks are exposed only in the southern part of the Maya block. West of the Tehuantepec isthmus, ~1 Ga old granulites of the Guichicovi complex resemble Grenville-age rocks from the Oaxacan complex that form the basement of the Zapoteco terrane (Figure 1, Weber and Köhler 1999; Ruiz *et al.*, 1999; Solari *et al.*, 2003). The Guichicovi complex is intruded mostly by Late Permian granitoids (Damon *et al.*, 1981; Murillo-Muñetón 1994; Weber 1998). East of the Tehuantepec isthmus, the Chiapas Massif encompasses more than 20,000 km² parallel to the Pacific coast. It is mainly composed of batholith-scale plutonic rocks and orthogneisses of Late Permian to Early Triassic age (Damon *et al.*, 1981; Schaaf *et al.*, 2002; Weber *et al.*, 2005). The metaigneous rocks are interlayered with metasedimentary rocks recording a medium- to high-grade metamorphism at ~250–254 Ma (Weber *et al.*, 2002, 2007). Repeatedly folded metamorphosed psammites, greywackes, calcsilicates, marbles, and minor metapelites are exposed in the northeastern part of the Chiapas Massif. These metasediments were referred to as "La Sepultura unit" (Weber *et al.*, 2002, 2007). In the central Chiapas Massif, anatectic garnet-amphibolite with lenses of calcsilicate and marble together with minor metapelites compose the "Custepec unit" that records peak metamorphic conditions of 9 kbar and probably >800 ºC (Estrada-Carmona *et al.*, 2009; Weber *et al.*, 2007). Internal correlations of the metasediments and provenance studies of the protoliths have turned out to be difficult. At least two sequences of sedimentary protoliths with different provenance patterns were involved in the Late Permian orogenic event. One part of metasedimentary protoliths probably correlates with late Paleozoic sediments of the Upper Santa Rosa Formation, others have Mesoproterozoic detrital zircon cores only (Weber *et al.*, 2007, 2008), and may correlate with lower Paleozoic sedimentary rocks from the Maya Mountains of Belize (Martens *et al.*, 2006) and central Guatemala (Solari *et al.*, in press).

Clemons and Burkart (1971) summarized several late Paleozoic sequences in Guatemala in the Santa Rosa Group which includes three formations (Figure 2): 1) the Chicol Formation, a sequence of conglomerates, sandstone with volcaniclastic and volcanic interbeds (Anderson *et al.*, 1985); 2) the middle Tactic Formation of Pennsylvanian-Permian age which is composed of shales, mudstone, minor siltstone and fine sandstone beds; and 3) limestones with interbedded fossiliferous shales, sandstones and dolomites of the Esperanza Formation of Wolfcampanian age. A detailed summary about the stratigraphy of the Santa Rosa Group, including all relevant references, is given by Weber *et al.* (2006).

In Chiapas, Paleozoic sedimentary rocks correlative with the Santa Rosa Group were described between

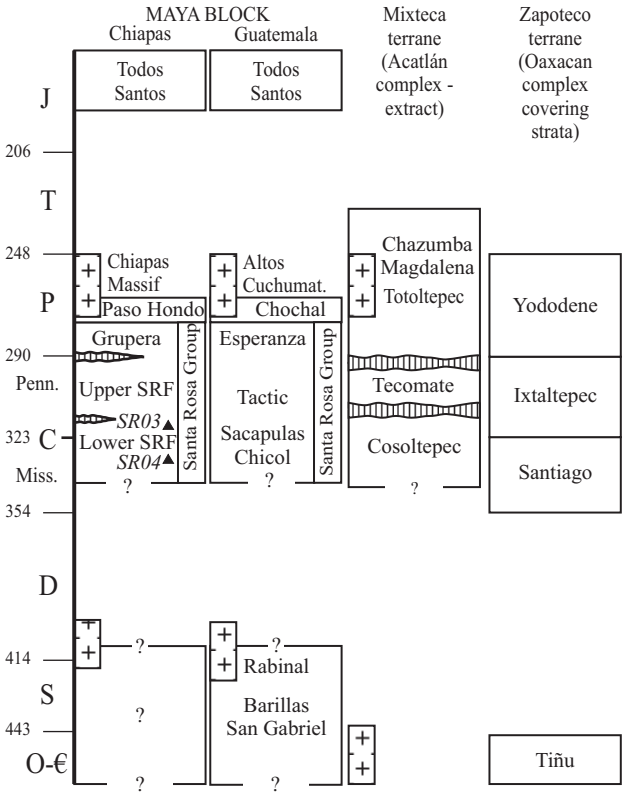

Figure 2. Simplified Paleozoic to Jurassic stratigraphic columns of the Maya block in Chiapas (modified from Hernández-Gracía, 1973) and Guatemala (adopted from Ortega-Gutiérrez *et al.*, 2007). For comparison, extracts from the stratigraphic columns of the Acatlán complex (from Keppie *et al.*, 2006) and the Zapoteco terrane (from Gillis *et al.*, 2005) are also shown.

Chicomuselo and La Concordia (Figure 3) and were subdivided into the Upper and the Lower Santa Rosa Formation (SRF) which are apparently separated by an angular unconformity (Hernández-García, 1973).

The Lower SRF was exclusively described in the "Río Aguacate" valley south of La Concordia (Figure 3) as a monotonous, 6300 m thick sequence of slate and phyllite with intercalated horizons of metaquartzites as thick as 20 cm, and a single quartz-clast conglomerate 10 m thick (Hernández-García, 1973). Based upon a fossiliferous horizon with Paleozoic crinoids, Hernández-García (1973) interpreted this sequence as being at least of Late Mississippian age. Its lower limit is nowhere exposed, but metamorphic conditions increase towards the base of the column from where small garnet crystals were reported (Hernández-García, 1973).

The Upper SRF comprises a voluminous (~5800 m; López-Ramos, 1979) sequence of flysch-type rocks of middle to upper Pennsylvanian age (Hernández-García, 1973) that is best exposed in the Chicomuselo area (Figure 3b). The Upper SRF is covered by siliceous shales and limestones (Grupera Formation), containing Early Permian (Wolfcampanian) fusulinids (Hernández-García, 1973; López-Ramos, 1979). The Grupera Formation correlates with the Esperanza Formation, which forms the uppermost part of the Santa Rosa Group in Guatemala (Figure 2). Fossiliferous gray limestones of Leonardian age (Paso Hondo Formation) conformably overlie the Grupera Formation southeast of Chicomuselo (Figure 3). These limestone beds are the uppermost Paleozoic sedimentary rocks in Chiapas and Guatemala and they are not part of the Santa Rosa Group (Figure 2; Clemons and Burkart, 1971).

The geologic relations between the SRF and late Paleozoic crystalline rocks of the Chiapas Massif are complex and still mostly unknown. Red beds of the Jurassic Todos Santos Formation cover an about 20 km wide strip between the SRF and the Chiapas Massif. On the other hand, Paleozoic metasedimentary rocks are shown on the geologic map by Jiménez-Hernández *et al.* (2005) in unspecified contact with gneisses at the SE part of the Chiapas Massif (Figure 3b). From this area, Pompa-Mera *et al.* (2007) reported Silurian to lower Devonian (392–413 Ma) Ar-Ar and Rb-Sr mica cooling ages from a phyllite, which was reheated by the intrusion of felsic granite. These data imply the existence of pre-SRF sedimentary rocks in the Chiapas Massif of at least Silurian age.

In Guatemala, in Los Altos Cuchumatanes (north of the Polochic Fault, Figure 1) the Santa Rosa Group is underlain by low- to high-grade metamorphic rocks (Barillas complex; Ortega-Gutiérrez *et al.*, 2007 and references therein) which are intruded by Permian and Early Devonian (391 ± 7 Ma) granites (Solari *et al.*, in press). South of the Polochic fault in the Baja Verapaz area of central Guatemala (Figure 1), conglomerates, shales, and limestones with Mississippian conodonts (Ortega-Obregón, 2005) cover clastic metasediments of the San Gabriel sequence (Ortega-Obregón, 2005; Solari *et al.*, in press). These metasediments are intruded by the S-type Rabinal granite of probable Silurian age (Figure 2; Ortega-Obregón, 2005).

In the Maya Mountains of Belize (Figure 1), Paleozoic sedimentary rocks have also been correlated with the Santa Rosa Group (Bateson and Hall, 1977). On the basis of U-Pb dating of detrital and igneous zircons, Martens *et al.* (2006) recognized at least two different sedimentary sequences in the Maya Mountains similar to those suggested by Dixon (1956): (1) a fossiliferous Pennsylvanian-Permian sequence resembling the Santa Rosa Group and (2) a sequence of at least Silurian to lower Devonian age with an ~410 Ma old interlayered tuff (Martens *et al.*, 2006).

THE LOWER SANTA ROSA FORMATION IN SOUTHERN MEXICO

Since Hernández-García (1973) defined the Lower SRF along the "Río Aguacate" river section, the Grijalva river was blocked by the La Angustura dam, and some areas south of La Concordia were flooded (Figures 3 and 4). Unfortunately, Hernández-García (1973) did not provide detailed geographic descriptions of the Río Aguacate location. Besides that, the present-day topographic maps available from INEGI and the recent geologic map by Servicio Geológico Mexicano (Jiménez-Hernández *et al.*, 2005) do not mention any river named "Río Aguacate". Therefore, it is not clear if this section was inundated or not. However, the only river that coincides with the description by Hernández-García (1973) is "Río Jaltenago", which drains from the Chiapas Massif across Jaltenango into the La Angostura lake (Figures 3 and 4). The historic geologic map of Chiapas (Sapper, 1899) shows phyllite and mica-schist in contact with a unit designated as Santa Rosa, and they are intersected by a river called "Aguacate" (Figure 3a). The "Aguacate" river on Sapper's map coincides almost perfectly with the "Río Jaltenango" on the current maps (Figure 3b). Therefore, we believe "Río Jaltenango" to be a synonym for "Río Aguacate", the latter being a historical name for the same river.

A branch of the La Angostura lake enters "Río Jaltenango" (Figure 3) valley from NE. Access is possible by boat from the village of Ignacio Zaragoza towards the SW (Figure 4). Yellowish brown sandstone of the Todos Santos Formation (Jurassic), plunging ~15º towards N-NE crops out along the west coast of the lake, southward from Ignacio Zaragoza. Upstream the "Río Jaltenango", the valley narrows and outcrops of grayish brown slate that dip moderately southward are exposed at 15º59.7' N; 92º36.2' W. Monotonous exposures of slate, siltstone, phyllite, and intercalated sandstone layers are exposed continuously along both flanks of the valley for the next 4 km (Figure 5a). The aspect of the outcrops matches perfectly with the description given by Hernández-García (1973). However, we did not find a 10 m thick quartz-conglomerate horizon

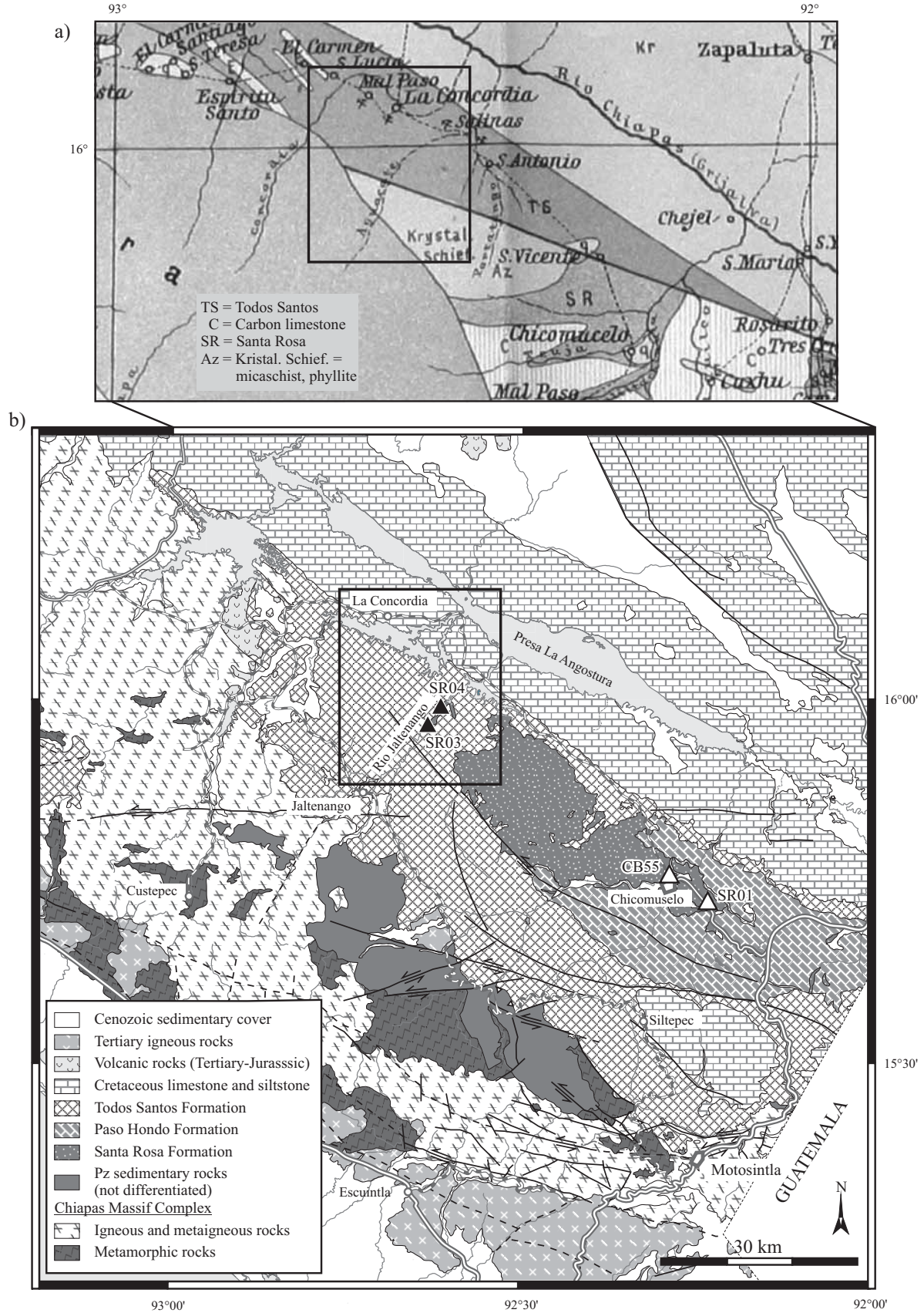

Figure 3. a: Cutout from the historical geologic map of Sapper (1899). b: Simplified geologic map of the study area (modified from Jiménez-Hernández *et al.*, 2005 and Martínez-Amador *et al.*, 2005), showing sample locations SR03 and SR04 from this work and SR01 and CB55 from Weber *et al.* (2006). Note: Black rectangle marks the same geographic area in both (a) and (b).

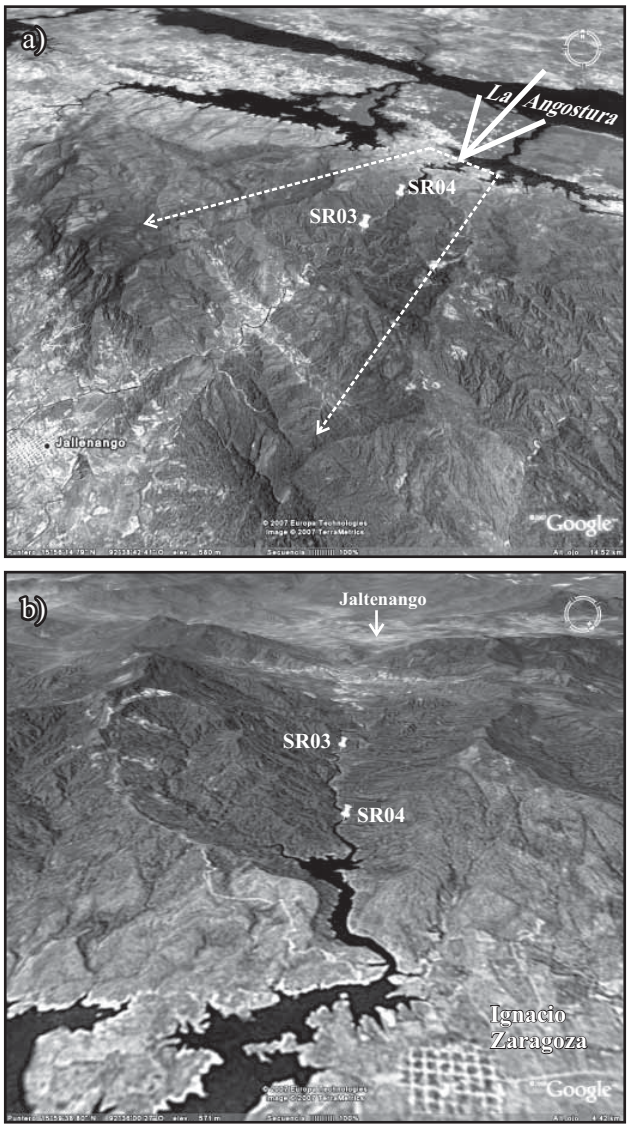

Figure 4. Satellite images (Google©) of the study area, showing the sample locations. a: Perspective overview looking from south to north with the La Angostura lake in the background; b: perspective view from NNW to SSE into the "Río Jaltenango" valley as indicated in (a).

or garnet-bearing schist that are described as present at the base of the sequence. We postulate that these are within the lowermost part of the sequence and are flooded.

SAMPLE LOCALITIES IN THE RÍO JALTENANGO VALLEY

Sample SR03

The southernmost accessible outcrop (SR03, Figure 4) comprises slightly metamorphosed siltstone, slate, and grayish clayey sandstone with cm-scale graded beds, suggestive of flysch-type sedimentation (Figure 5b). Our sample SR03 is from a sandy layer within this graded sequence that dips 75º towards the SSW (200). The layer is composed of fine-grained quartz, concentrated in quartz-rich bands, or lithic fragments with minor feldspar (perthite and plagioclase). Grading is also visible in thin section as the abundance of quartz grains changes continuously into layers dominated by finer-grained chlorite, white mica, and opaque minerals. Layers rich in phyllosilicates define the schistosity and a secondary crenulation cleavage, forming a mesh structure. Deformation is also shown by oriented elongate quartz with undulose extinction, chlorite fibers in the pressure shadows of larger quartz grains and of opaque minerals. Fibrolithic chlorite and white mica together with carbonate are secondary phases that indicate low grade metamorphic overprint. Zircons and tourmaline are accessory minerals.

Sample SR4

Sample SR04 is from an outcrop close to the northernmost exposure of the sequence (Figure 4). The beds dip moderately south and they are cut by penetrative cleavage dipping 30º southeast (~155) (Figure 5c). Provided that the sequence is not inverted and/or repeated by folding or faulting, the northern outcrops must be stratigraphically lower than the outcrops further south. By assuming that the dip of the beds rises continuously from 40º (SR04) to 60º (SR03) towards the S-SW, a thickness of approximately 3000 m can be estimated from outcrop SR03 near the top to outcrop SR04 near the base of the exposed sequence.

Sample SR04 is taken from a low grade metamorphosed quartzose sandstone layer. Bands of orthoquartzite with polygonal texture fade into bands with (<0.5 mm) rounded quartz grains, having undulose extinction and subgrain boundaries in a very fine-grained matrix of chlorite, small quartz (recrystallized?), white mica, and minor plagioclase in the matrix. Accessory tourmaline forms radial patterns and zircons are more abundant in SR04 than in SR03.

METHODS

Samples were crushed, milled and sieved at the Instituto de Geología at UNAM. Zircons were separated from the <80 mesh fraction by standard procedures at the Geology Department at CICESE by using a Wilfley® table, a Frantz® isodynamic separator, heavy liquids, and hand-picking techniques.

Laser-ablation multicollector ICP MS was conducted following the method described by Gehrels *et al.* (2006). Zircon crystals were analyzed with a Micromass Isoprobe multicollector ICP MS linked to a New Wave ArF Excimer laser ablation system at the University of Arizona, Tucson AZ, which has an emission wavelength of 193 nm. The collector configuration allows measurement of ^{204}Pb with an ion-counting channel, whereas ^{206}Pb, ^{207}Pb, ^{208}Pb, ^{232}Th and

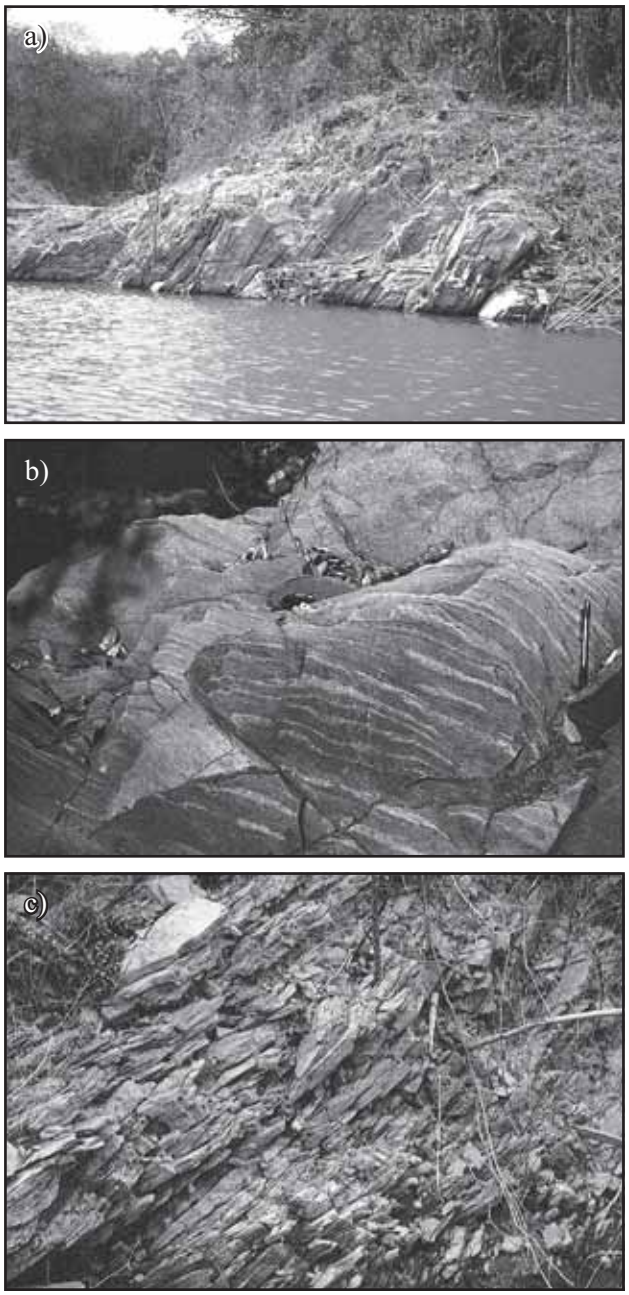

Figure 5. a: Outcrop of the Lower Santa Rosa Formation protruding above the lake in the flooded "Río Jaltenango" valley (beds are dipping southward). b: Graded flysch-like bedding at cm-scale of the Santa Rosa Formation at outcrop SR03. c: Penetrative foliation cutting the slaty cleavage at a low angel at outcrop SR04.

^{238}U were measured simultaneously with Faraday detectors. All analyses were conducted in static mode with a laser beam diameter of 35 µm, operated with output energy of ~32 mJ (at 23 kV) and a pulse rate of 8 Hz. Each analysis consisted of one 12-second integration on peaks without laser firing for backgrounds and twelve 1-second integrations on peaks with the laser firing. Hg contribution to the ^{204}Pb mass position was removed by subtracting on-peak background values. Inter-element fractionation was monitored by analyzing an in-house zircon standard which has a concordant ID-TIMS age of 563.5 ± 3.2 Ma (2σ) (Gehrels *et al.*, 2008). This standard was analyzed once for every five unknown zircon grains. Uranium and Thorium concentrations were monitored by analyzing a standard (NIST 610 Glass) with ~500 ppm Th and U. The lead isotopic ratios were corrected for common Pb, using the measured ^{204}Pb, assuming an initial Pb composition according to Stacey and Kramers (1975) and respective uncertainties of 1.0, 0.3 and 2.0 for ^{206}Pb/^{204}Pb, ^{207}Pb/^{204}Pb, and ^{208}Pb/^{204}Pb. The age probability plots (Ludwig, 2003) were based upon the ^{206}Pb/^{238}U age for young (<0.9 Ga) zircons and the ^{207}Pb/^{206}Pb age for older (>0.9 Ga) grains. This division at 0.9 Ga was chosen because of the increasing uncertainty of ^{206}Pb/^{238}U ages and the decreasing uncertainty of ^{207}Pb/^{206}Pb ages as a function of age.

RESULTS

SR03

Most zircons of sample SR03 are rounded, oval, or drusy due to abrasion during sediment transport, and do not exceed 50 microns. Few grains are prismatic, up to 100 microns long with ~1:3 aspect ratios, but their pyramidal tips show abrasion. Some grains are dark pinkish colored others are clear. We analyzed U-Th-Pb isotope ratios of 100 grains. The data are listed in Table 1 and illustrated on concordia diagrams (Figure 6a) and combined relative probability-histogram plots (Figure 6b). Four grains have Archaean ^{207}Pb/^{206}Pb ages (2807–2662 Ma) and 11 yielded Paleoproterozoic ^{207}Pb/^{206}Pb ages (2338–1695 Ma) with a notable probability peak of concordant zircons at ~2118 Ma. A group of four grains (1590–1525 Ma) defines a small probability peak at ~1550 Ma and another three grains are slightly younger (1481–1366 Ma). Another group of four grains yields early Mesoproterozoic ^{207}Pb/^{206}Pb ages from ~1256 to ~950 Ma.

The oldest group of five Neoproterozoic zircons has ^{206}Pb/^{238}U ages from ~891 to ~701 Ma with a probability peak at ~885 Ma which is defined by two concordant grains. The majority of 55 grains have ^{206}Pb/^{238}U ages in the range from 700 to 500 Ma. Within this range of zircon ages, probability peaks of two potential sources can be distinguished; one at ~611 Ma and another one at ~568–555Ma. Slightly older grains with a peak at ~690 Ma may also be significant.

Most of the zircons younger than 530 Ma (14 out of 21) are either more than 20% discordant or more than 10% negative discordant, thus any interpretation of these data must be considered with care. Usually we omit such data from the probability plots (Figure 6b). However, LA-MC-ICPMS measurements of Phanerozoic zircons commonly have low ^{207}Pb signals leading to high analytical errors in ^{207}Pb/^{206}Pb ratios. In such cases, the greater discordance is

Table 1. LA-MC-ICPMS U-Th-Pb data of detrital zircons from silty sandstone SR03, Lower Santa Rosa Formation, La Concordia, Chiapas. (Long. 92.6258º W, Lat. 15.9665º N).

Grain-spot	U ppm	$^{206}Pb/^{204}Pb_c$	$^{232}Th/^{238}U$	$^{207}Pb^*/^{235}U$ ± 1σ %		$^{206}Pb^*/^{238}U$ ± 1σ %		Err corr	Apparent ages					
									$^{206}Pb/^{238}U$ (Ma) ±1σ		$^{207}Pb/^{235}U$ (Ma) ±1σ		$^{207}Pb/^{206}Pb$ (Ma) ±1σ	
(1)				(2)		(2)			(3)				(3)	
SR03-1	319	4484	0.9	0.78033	6.2	0.09277	1.3	0.21	**571.9**	7.3	585.7	27.6	639.3	130.5
SR03-2	301	4719	2.4	0.78033	6.2	0.09277	1.3	0.21	**571.9**	7.3	585.7	27.6	639.3	130.5
SR03-3	145	2083	0.8	0.77870	5.3	0.09312	4.0	0.76	**573.9**	22.2	584.7	23.5	626.9	73.7
SR03-4	105	3162	1.0	0.58604	7.2	0.07587	3.2	0.45	**471.4**	14.6	468.3	27.0	453.2	143.0
SR03-4A	273	17003	0.6	14.98239	8.8	0.54971	8.2	0.93	2824.0	187.5	2814.1	84.4	**2807.1**	54.5
SR03-5	689	33684	8.0	6.66182	4.9	0.37996	3.7	0.76	2076.1	66.1	2067.6	43.5	**2059.1**	56.8
SR03-6	116	4201	0.7	14.45707	5.3	0.54719	1.3	0.24	2813.5	28.5	2780.2	50.4	**2756.1**	84.7
SR03-7	213	2726	0.7	3.54102	8.1	0.27071	4.6	0.57	1544.4	63.2	1536.4	64.5	**1525.4**	126.5
SR03-8	756	8673	3.0	0.81854	3.6	0.09866	1.4	0.38	**606.6**	7.8	607.2	16.2	609.7	71.1
SR03-9	403	6298	1.1	0.84520	3.7	0.10308	1.6	0.43	**632.5**	9.7	622.0	17.2	584.2	72.4
SR03-11	146	1837	10.7	0.97848	3.9	0.11344	1.3	0.32	**692.7**	8.3	692.8	19.6	693.2	78.9
SR03-12	85	1177	0.4	0.72044	5.8	0.08577	2.9	0.50	**530.5**	14.8	550.9	24.7	636.4	108.4
SR03-13	180	3402	1.1	0.72825	6.4	0.08544	2.9	0.46	**528.5**	14.9	555.5	27.2	667.8	121.0
SR03-14	61	803	1.0	1.00232	2.9	0.11491	1.6	0.54	**701.2**	10.5	705.0	14.9	717.0	52.5
SR03-15	424	6988	0.8	0.76484	5.5	0.09181	2.2	0.40	**566.3**	11.8	576.8	24.3	618.5	109.4
SR03-16	625	7713	4.0	0.99757	4.0	0.11220	2.8	0.69	**685.5**	18.0	702.6	20.4	757.4	61.8
SR03-17	249	3621	2.3	0.69218	5.5	0.08444	4.7	0.86	**522.6**	23.5	534.1	22.8	583.7	61.7
SR03-18	181	6432	2.3	0.80069	4.8	0.09031	2.0	0.42	**557.4**	10.8	597.2	21.7	751.6	92.0
SR03-19	410	3809	0.7	2.57125	4.4	0.22619	1.0	0.23	1314.5	11.9	1292.5	32.4	**1256.1**	84.6
SR03-20	287	3430	1.2	0.91465	7.1	0.10281	2.3	0.33	**630.9**	14.0	659.5	34.3	758.8	140.7
SR03-21	178	2222	0.9	0.55599	4.7	0.07040	2.1	0.45	**438.6**	9.0	448.9	17.1	502.2	92.5
SR03-22	758	10781	13.9	0.70533	6.4	0.08294	2.0	0.31	**513.6**	9.7	542.0	26.7	663.0	129.5
SR03-23	431	5057	1.0	0.91447	3.5	0.10580	2.7	0.79	**648.3**	16.9	659.4	16.8	697.6	45.5
SR03-24	57	1377	0.8	0.82391	2.9	0.09930	1.6	0.56	**610.3**	9.5	610.2	13.3	609.9	51.7
SR03-25	68	1011	0.8	1.39223	6.6	0.14577	3.3	0.51	**877.2**	27.4	885.6	39.0	906.8	117.1
SR03-26	608	5045	1.0	1.05046	4.6	0.10346	2.3	0.49	**634.7**	13.8	729.1	24.2	1031.6	81.9
SR03-27	370	30045	1.0	0.52310	8.3	0.06575	3.0	0.37	**410.5**	12.1	427.2	28.8	518.4	168.9
SR03-28	111	4709	0.9	14.20366	2.9	0.52479	1.6	0.56	2719.4	36.1	2763.4	27.4	**2795.7**	39.1
SR03-30	1777	9899	29.0	4.26097	2.7	0.29739	2.5	0.89	1678.4	36.2	1685.9	22.5	**1695.2**	22.6
SR03-31	200	3197	1.7	5.28304	6.1	0.31874	5.5	0.91	1783.6	86.1	1866.1	51.7	**1959.4**	44.1
SR03-32	270	2862	0.4	0.87858	9.8	0.10676	3.1	0.32	**653.9**	19.4	640.2	46.4	592.1	200.9
SR03-33	238	4194	1.8	0.92264	4.4	0.10415	3.5	0.80	**638.7**	21.5	663.8	21.5	749.8	55.9
SR03-34	157	1194	0.4	1.22018	3.1	0.13020	2.8	0.92	**789.0**	20.9	809.9	17.1	867.7	24.8
SR03-35	251	12880	8.3	0.46314	8.0	0.06110	4.1	0.51	**382.3**	15.2	386.4	25.6	411.3	153.2
SR03-36	251	3423	0.9	7.62792	7.1	0.41167	4.4	0.62	2222.6	82.8	2188.2	63.8	**2156.0**	97.3
SR03-37	320	4370	1.0	0.82435	6.7	0.09585	5.7	0.85	**590.1**	32.1	610.5	30.8	686.9	75.8
SR03-38	323	3563	0.9	0.86214	7.0	0.10235	4.4	0.63	**628.2**	26.4	631.3	32.9	642.4	116.9
SR03-39	201	2697	0.6	0.62541	6.1	0.08104	4.1	0.67	**502.3**	19.7	493.2	23.7	451.3	99.7
SR03-40	165	2201	1.6	0.81782	4.2	0.09932	3.3	0.78	**610.4**	19.1	606.8	19.3	593.5	57.6
SR03-41	389	5055	4.4	0.77373	6.0	0.09449	2.6	0.43	**582.0**	14.3	581.9	26.7	581.4	118.5
SR03-42	297	4268	1.1	0.82427	4.8	0.10057	4.5	0.94	**617.8**	26.7	610.4	22.2	583.2	36.4
SR03-43	145	2001	2.6	0.76132	2.9	0.09390	1.7	0.59	**578.6**	9.4	574.8	12.8	559.8	51.4
SR03-44	264	2800	2.8	0.73046	7.8	0.08925	5.1	0.65	**551.1**	26.9	556.8	33.4	580.2	127.9
SR03-45	219	6974	1.9	0.52443	3.7	0.06926	3.0	0.80	**431.7**	12.4	428.1	13.0	408.8	49.4
SR03-46	208	2024	1.2	2.28440	4.3	0.20674	3.4	0.81	1211.4	38.0	1207.5	30.1	**1200.4**	49.5
SR03-47	145	1999	6.5	0.50258	5.9	0.06789	3.9	0.66	**423.4**	16.0	413.4	19.9	358.2	99.0
SR03-48	539	29388	4.8	0.89312	4.1	0.10007	2.6	0.63	**614.8**	15.1	648.0	19.5	765.6	66.6
SR03-49	225	4488	2.1	12.40035	3.4	0.49700	2.5	0.73	2600.9	53.7	2635.2	32.2	**2661.6**	38.6
SR03-50	195	3571	0.9	0.86720	7.5	0.09938	2.3	0.31	**610.8**	13.4	634.0	35.2	717.8	150.8
SR03-51	199	7947	1.4	0.99481	6.2	0.11682	3.7	0.59	**712.2**	24.8	701.2	31.5	665.9	107.5
SR03-52	359	5988	4.2	6.53538	5.3	0.36265	2.5	0.48	1994.7	43.7	2050.7	46.6	**2107.4**	81.5
SR03-53	95	979	1.0	0.92516	3.3	0.10996	2.5	0.77	**672.5**	16.2	665.1	16.0	639.9	44.9
SR03-54	259	9012	1.6	0.42305	6.2	0.05722	3.3	0.52	**358.7**	11.3	358.2	18.7	355.3	119.4
SR03-55	281	14103	2.4	4.46767	5.2	0.30222	4.7	0.92	1702.3	70.9	1725.0	42.8	**1752.6**	37.3
SR03-56	140	1791	0.7	6.92629	3.5	0.38629	2.4	0.68	2105.6	42.5	2102.0	31.0	**2098.5**	45.0
SR03-57	294	3884	2.0	0.76238	3.3	0.09419	2.0	0.60	**580.3**	11.1	575.4	14.6	556.1	58.1
SR03-58	683	4663	0.8	0.84503	4.4	0.10023	3.2	0.75	**615.8**	19.1	621.9	20.2	644.3	62.2
SR03-59	133	2136	0.9	0.39041	5.8	0.05001	2.6	0.45	**314.6**	8.0	334.7	16.7	476.8	115.6
SR03-60	351	10827	0.5	0.86425	4.2	0.10370	2.7	0.65	**636.1**	16.6	632.4	20.0	619.5	70.0
SR03-61	153	1795	0.7	2.83210	4.1	0.23548	3.4	0.83	1363.1	41.6	1364.1	30.6	**1365.5**	43.9

Table 1 (Continued). LA-MC-ICPMS U-Th-Pb data of detrital zircons from silty sandstone SR03, Lower Santa Rosa Formation, La Concordia, Chiapas. (Long. 92.6258º W, Lat. 15.9665º N).

Grain-spot	U ppm	$^{206}Pb/^{204}Pb_c$	$^{232}Th/^{238}U$	$^{207}Pb^*/^{235}U$ ± 1σ %		$^{206}Pb^*/^{238}U$ ± 1σ %		Err corr	Apparent ages $^{206}Pb/^{238}U$ (Ma) ±1σ		$^{207}Pb/^{235}U$ (Ma) ±1σ		$^{207}Pb/^{206}Pb$ (Ma) ±1σ	
(1)				(2)		(2)			(3)				(3)	
SR03-62	910	8261	2.4	0.72932	6.4	0.08916	3.6	0.57	**550.6**	19.1	556.2	27.2	579.1	113.6
SR03-63	185	2407	0.8	0.53313	2.5	0.06615	1.8	0.71	**412.9**	7.1	433.9	8.9	546.7	38.9
SR03-64	501	6692	0.6	0.71357	3.5	0.08933	2.5	0.72	**551.6**	13.2	546.9	14.6	527.3	52.3
SR03-65	370	14857	9.7	0.75077	5.0	0.09291	3.0	0.61	**572.7**	16.7	568.7	21.9	552.6	87.4
SR03-66	351	2364	0.8	9.23458	4.6	0.44847	2.1	0.46	2388.5	41.9	2361.5	41.7	**2338.4**	69.2
SR03-67	367	13312	2.4	0.74743	6.9	0.09085	2.9	0.42	**560.6**	15.6	566.7	29.9	591.5	135.3
SR03-68	373	4879	0.7	2.88139	3.8	0.23514	1.7	0.44	1361.4	20.6	1377.1	28.5	**1401.4**	64.8
SR03-69	246	3043	0.8	0.71276	4.1	0.08670	2.8	0.70	**536.0**	14.5	546.4	17.1	590.0	63.0
SR03-70	184	2223	1.0	0.78202	6.7	0.09133	1.4	0.22	**563.4**	7.8	586.6	29.7	677.7	139.0
SR03-71	376	5752	1.2	0.50824	3.4	0.06506	3.0	0.88	**406.3**	12.0	417.3	11.8	478.2	35.8
SR03-72	483	18072	4.0	0.81930	4.3	0.09693	2.6	0.59	**596.4**	14.5	607.7	19.9	649.9	75.6
SR03-73	305	12258	16.5	3.52802	2.5	0.26968	1.5	0.59	1539.2	20.2	1533.5	19.9	**1525.7**	38.5
SR03-74	145	7251	1.7	3.47209	2.9	0.26535	1.7	0.60	1517.2	23.6	1520.9	23.0	**1526.1**	44.0
SR03-75	416	5352	1.1	6.92358	3.2	0.38386	2.7	0.83	2094.3	47.4	2101.7	28.5	**2108.9**	31.6
SR03-76	294	2049	0.3	0.73087	3.5	0.08928	1.9	0.56	**551.3**	10.3	557.1	14.9	580.7	62.6
SR03-77	294	2480	0.4	0.36695	5.5	0.05175	3.9	0.72	**325.3**	12.5	317.4	15.0	259.9	88.1
SR03-78	50	1330	0.6	0.42730	5.6	0.05860	3.6	0.64	**367.1**	13.0	361.3	17.1	323.7	97.8
SR03-79	272	10324	1.5	1.69466	3.6	0.16624	2.3	0.63	991.4	20.7	1006.5	22.9	**1039.7**	56.4
SR03-80	218	2675	0.6	3.10869	6.4	0.24333	5.3	0.83	1404.0	67.4	1434.8	49.2	**1480.9**	67.1
SR03-81	397	10632	0.6	0.64000	4.8	0.08358	1.9	0.39	**517.5**	9.4	502.3	19.1	433.8	98.9
SR03-82	526	8094	12.4	1.39102	2.6	0.14818	1.1	0.42	**890.8**	9.0	885.1	15.3	871.1	48.8
SR03-83	198	2748	4.3	0.83748	3.5	0.09915	1.8	0.52	**609.4**	10.7	617.8	16.4	648.4	65.2
SR03-84	280	3981	1.1	0.73967	4.2	0.08926	2.3	0.53	**551.1**	11.9	562.2	18.3	607.3	77.3
SR03-85	219	4912	1.0	0.84501	4.2	0.10065	2.9	0.69	**618.2**	17.3	621.9	19.7	635.3	65.5
SR03-86	123	1926	0.4	1.62845	5.2	0.16694	3.1	0.60	995.2	28.8	981.3	32.7	**950.1**	85.0
SR03-87	374	4996	1.1	0.71721	3.1	0.08878	1.2	0.37	**548.3**	6.1	549.0	13.2	552.0	63.3
SR03-88	173	2509	0.7	0.88190	3.6	0.10150	1.4	0.40	**623.2**	8.5	642.0	17.1	708.8	70.2
SR03-89	113	1579	0.4	0.73969	3.8	0.08969	2.5	0.65	**553.7**	13.3	562.2	16.6	596.8	63.2
SR03-90	87	1129	0.9	0.76463	4.6	0.09059	2.5	0.55	**559.0**	13.4	576.7	20.1	646.9	81.8
SR03-91	587	35048	1.3	0.73231	6.8	0.08515	5.6	0.81	**526.8**	28.2	557.9	29.4	687.0	84.7
SR03-92	962	869	1.2	7.68372	5.0	0.40733	3.9	0.78	2202.7	73.0	2194.7	44.9	**2187.2**	53.9
SR03-93	123	1679	0.6	0.63305	5.7	0.06686	2.9	0.50	**417.2**	11.6	498.0	22.5	888.8	101.9
SR03-94	250	2232	0.7	0.62262	8.0	0.08095	4.1	0.51	**501.8**	19.8	491.5	31.3	443.6	153.9
SR03-95	136	2346	0.8	0.39051	5.2	0.05078	1.3	0.25	**319.3**	4.1	334.7	14.8	443.6	112.1
SR03-96	320	4786	0.4	0.94173	9.0	0.11467	5.4	0.60	**699.8**	35.9	673.8	44.3	587.8	155.7
SR03-97	198	2776	1.4	0.81529	2.3	0.09649	1.8	0.78	**593.8**	10.1	605.4	10.5	649.1	30.9
SR03-98	463	22043	1.3	0.79242	3.5	0.09191	2.8	0.82	**566.8**	15.5	592.5	15.7	692.2	43.0
SR03-98A	391	4868	0.7	5.89345	6.0	0.35735	5.2	0.87	1969.6	88.9	1960.3	52.1	**1950.4**	52.0
SR03-99	127	1946	1.2	0.76141	5.8	0.09295	5.6	0.96	**573.0**	30.8	574.8	25.5	582.1	33.5
SR03-100	184	8458	0.5	0.85267	6.4	0.10001	5.0	0.79	**614.5**	29.4	626.1	29.7	668.4	83.5

(1) Sample identifier–spot number; (2) Isotope ratios corrected for common Pb using measured ^{204}Pb for correction. Individual errors are given as 1 sigma standard deviation; (3) Most reliable apparent ages are indicated in **bold**. Note: If the average of apparent ages is mid-Proterozoic and older (>900 Ma) then $^{207}Pb/^{206}Pb$ ages are considered as most reliable apparent ages; for younger values $^{206}Pb/^{238}U$ ages are used.

not relevant if the relative error in $^{207}Pb/^{206}Pb$ is larger than the percent of discordance. Therefore, the $^{206}Pb/^{238}U$ age, which is the more reliable apparent age for younger zircons, may be a meaningful value, assuming that Pb-loss is negligible and that the laser sampled only a single age domain within the zircon crystal. Considering these $^{206}Pb/^{238}U$ ages, seven grains defined an additional probability peak at ~415 Ma (Figure 6b), and another three grains yielded Devonian (383–359 Ma) $^{206}Pb/^{238}U$ ages. The youngest cluster of three grains have $^{206}Pb/^{238}U$ ages from 325 ± 13 to 315 ± 8 (Table 1), defining a probability peak at ~318 Ma. This is a significant group of zircons with overlapping errors (Figure 6a) that fulfills the requirements for a robust source age as suggested by Gehrels *et al.* (2006).

SR04

SR04 contains zircons similar to those from SR03. Most zircons are rounded and smaller than 50 microns but, with respect to SR03, SR04 also contains larger, short- to long prismatic zircons with aspect ratios up to 5:1, and more grains with prism faces or soccer ball forms.

A total of 109 zircons were analyzed from sample

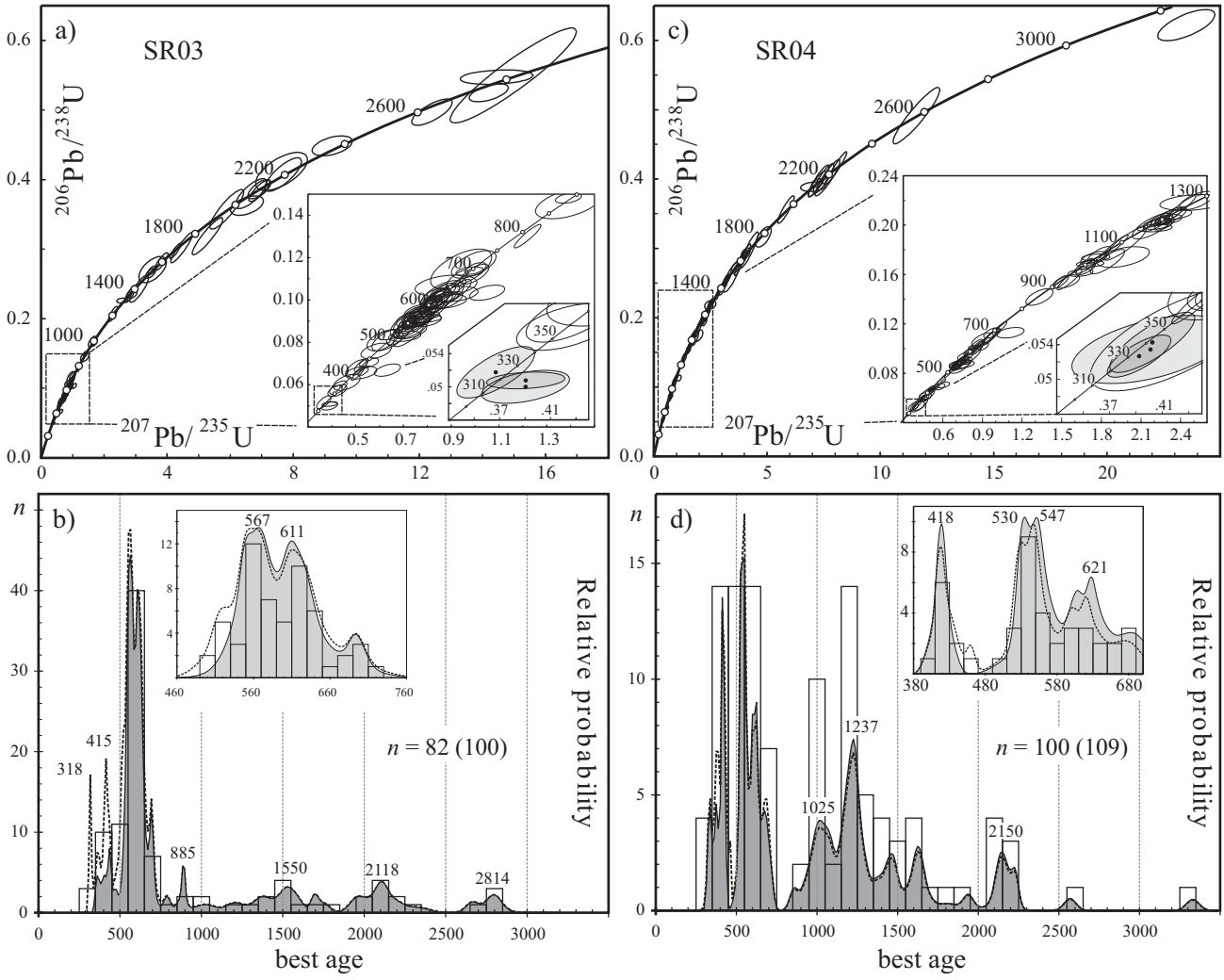

Figure 6. Concordia diagrams (a, c), relative age probability and histogram plots of best ages (b, d) for U-Pb isotope ratios of zircons from (a, b) sample SR03 and (c, d) sample SR04. Grey error ellipses in small amplified concordia plots in (a) and (c) were taken for concordia age calculations of the youngest age groups (dark grey with white border is the 2σ concordia age error ellipse calculated with Isoplot, Ludwig, 2003). Histograms show number of analysis within each 100 Ma interval; filled curves calculated from *n* = number of analysis with <20% discordance and <10% negative discordance. Dotted line includes also discordant data (*n* in brackets).

SR04 and only nine are either more than 20% discordant or more than 10% negatively discordant. The results are listed in Table 2 and plotted on a concordia diagram (Figure 6c) and combined relative probability-histogram plots (Figure 6d). Only two Archaean grains were detected; one concordant grain at 2569 ± 38 Ma (1σ) and another 6% discordant grain with a $^{207}Pb/^{206}Pb$ age of 3330 ± 41 Ma (1σ). Paleoproterozoic zircons (2232–1619 Ma) are more abundant (14 grains), having a significant probability peak at ~2150 Ma. Thirty nine zircon grains have Mesoproterozoic ages, of which the most prominent probability peak is at ~1237 Ma and a second, less pronounced peak at ~1025 Ma (Figure 6d). A group of seven grains range from ~1543 to ~1374 Ma. Neoproterozoic to Cambrian zircons are represented by a total of 34 grains, of which the oldest concordant one has a $^{206}Pb/^{238}U$ age of 855 ± 25 Ma (1σ). The zircons in the range from 700 to 500 Ma have a major probability peak at ~547–530 Ma and a minor peak at ~621 Ma. A group of seven reliable grains define a Silurian age peak at ~418 Ma and a group of Devonian (~390–371 Ma) zircons are also present. The three youngest zircons have $^{206}Pb/^{238}U$ ages from 341 ± 15 to 331 ± 10 (Table 2). Isotope ratios of this cluster of ages overlap within their errors (Figure 6c), recording a robust source age (see above; Gehrels *et al.*, 2006) with a probability peak at ~335 Ma.

DISCUSSION

Depositional age of the Lower Santa Rosa Formation

The maximum age of deposition of the beds from the lowermost outcrop SR04 is defined by the youngest detrital zircons with an age of ~335 Ma whereas at SR03

Table 2. LA-MC-ICPMS U-Th-Pb data of detrital zircons from silty sandstone SR04, Lower Santa Rosa Formation, La Concordia, Chiapas. (Long. 92.6075º W, Lat. 15.9890º N).

Grain-spot	U ppm	$^{206}Pb/^{204}Pb_c$	$^{232}Th/^{238}U$	$^{207}Pb^*/^{235}U$ ± 1σ %		$^{206}Pb^*/^{238}U$ ± 1σ %		Err corr	Apparent ages					
									$^{206}Pb/^{238}U$ (Ma) ±1σ		$^{207}Pb/^{235}U$ (Ma) ±1σ		$^{207}Pb/^{206}Pb$ (Ma) ±1σ	
(1)				(2)		(2)			(3)				(3)	
SR04-1	402	8064	1.1	0.70155	4.3	0.08661	2.1	0.49	**535.5**	10.9	539.7	18.2	557.7	82.6
SR04-3	158	5523	0.8	1.97857	5.4	0.18502	4.8	0.89	1094.3	48.4	1108.2	36.6	**1135.6**	49.8
SR04-3A	129	3179	4.1	0.73307	4.1	0.08851	2.0	0.49	**546.7**	10.5	558.4	17.5	606.0	76.7
SR04-4	259	8208	0.8	0.87186	2.8	0.10302	2.0	0.73	**632.1**	12.2	636.6	13.1	652.5	40.2
SR04-5	532	9140	3.5	0.51839	3.5	0.06634	2.6	0.72	**414.0**	10.3	424.1	12.3	479.0	53.9
SR04-6	449	9483	6.0	0.50790	1.7	0.06615	1.0	0.59	**412.9**	4.0	417.0	5.8	440.0	30.8
SR04-7	61	1947	1.3	0.74635	6.7	0.08806	3.9	0.58	**544.1**	20.4	566.1	29.3	655.7	118.0
SR04-8	60	1876	1.5	0.72984	6.8	0.08575	4.5	0.67	**530.4**	22.9	556.5	29.0	664.6	108.1
SR04-9	707	38820	2.8	2.20016	1.6	0.20155	1.0	0.61	1183.6	10.8	1181.1	11.5	**1176.5**	25.7
SR04-10	133	2524	2.2	0.77353	3.4	0.08892	1.4	0.41	**549.1**	7.3	581.8	15.1	711.3	66.1
SR04-11	186	12152	2.5	2.20346	4.0	0.19761	1.0	0.25	1162.5	10.6	1182.1	28.1	**1218.3**	76.8
SR04-12	142	2817	0.8	0.76656	4.8	0.09375	2.2	0.47	**577.7**	12.2	577.8	20.9	578.3	91.5
SR04-13	358	7731	0.8	0.69413	2.5	0.08479	1.3	0.52	**524.6**	6.6	535.3	10.5	580.9	46.6
SR04-14	764	43538	18.4	1.75825	4.1	0.17382	1.0	0.25	1033.1	9.8	1030.2	26.4	**1024.0**	80.0
SR04-14A	83	5184	2.1	2.52179	3.4	0.21989	2.2	0.66	1281.3	25.9	1278.3	24.8	**1273.3**	50.2
SR04-15	451	6474	1.8	0.50153	3.4	0.06449	2.3	0.69	**402.9**	9.1	412.7	11.4	468.1	53.8
SR04-16	138	3146	2.8	0.58010	4.1	0.06895	2.4	0.60	**429.8**	10.1	464.5	15.2	640.0	70.2
SR04-17	52	3969	2.8	3.09756	2.6	0.24704	1.2	0.46	1423.2	15.4	1432.1	20.0	**1445.3**	43.9
SR04-17A	98	3310	1.3	0.90510	3.0	0.10160	2.0	0.64	**623.8**	11.6	654.4	14.7	761.7	49.1
SR04-18	256	7071	0.7	0.80938	3.3	0.09793	2.2	0.66	**602.3**	12.4	602.1	14.9	601.5	53.8
SR04-19	393	17855	3.9	1.71563	4.0	0.16869	1.0	0.25	1004.9	9.3	1014.4	25.8	**1035.0**	78.6
SR04-19A	405	9635	3.7	0.51365	3.0	0.06721	1.0	0.34	**419.3**	4.1	420.9	10.3	429.5	62.5
SR04-20	275	16022	1.8	1.68226	2.9	0.16469	2.0	0.69	982.8	18.1	1001.8	18.3	**1043.8**	41.6
SR04-20A	249	8432	1.8	0.84636	4.2	0.10103	1.0	0.24	**620.4**	5.9	622.6	19.5	630.6	87.6
SR04-21	140	9464	2.4	2.25869	1.6	0.20389	1.0	0.63	1196.2	10.9	1199.5	11.2	**1205.4**	24.4
SR04-21A	310	8707	3.3	0.69354	4.2	0.08548	1.5	0.35	**528.7**	7.5	534.9	17.6	561.4	86.4
SR04-22	113	10903	1.7	3.59584	3.4	0.27237	2.1	0.63	1552.8	29.1	1548.6	26.7	**1542.9**	49.1
SR04-23	198	11498	2.2	1.64203	3.9	0.16136	1.2	0.31	964.3	10.6	986.5	24.4	**1036.1**	74.2
SR04-24	118	9249	1.7	3.12231	3.6	0.25018	3.1	0.86	1439.4	39.9	1438.2	27.5	**1436.4**	34.4
SR04-25	15	1048	2.0	1.96422	6.7	0.17415	3.2	0.47	1034.9	30.5	1103.3	45.3	**1240.8**	116.1
SR04-26	157	4609	2.0	0.74126	2.6	0.08872	1.2	0.44	**547.9**	6.1	563.1	11.3	625.0	50.6
SR04-27	244	5801	1.4	0.51964	2.5	0.06737	1.5	0.60	**420.3**	6.2	424.9	8.8	449.9	45.3
SR04-28	275	7674	0.6	0.71789	3.1	0.08658	2.5	0.81	**535.3**	13.0	549.4	13.3	608.5	39.4
SR04-29	62	3717	1.6	1.55934	4.0	0.15611	3.6	0.91	935.1	31.7	954.2	24.8	**998.5**	33.7
SR04-30	137	3760	1.1	0.68756	2.2	0.08506	1.6	0.71	**526.2**	7.9	531.3	9.1	553.3	33.8
SR04-31	114	17119	1.2	7.22265	2.3	0.39427	1.0	0.43	2142.6	18.2	2139.3	20.5	**2136.1**	36.2
SR04-32	449	31509	3.0	2.22756	3.3	0.20065	1.3	0.41	1178.8	14.5	1189.7	23.1	**1209.6**	59.3
SR04-33	90	2949	1.3	0.86214	3.3	0.09943	3.0	0.89	**611.1**	17.4	631.3	15.7	704.4	32.4
SR04-34	252	5009	0.9	0.50807	4.0	0.06698	2.9	0.72	**417.9**	11.6	417.1	13.7	412.7	62.6
SR04-35	57	3061	1.3	1.53897	4.1	0.15434	2.3	0.56	925.2	19.9	946.1	25.5	**994.9**	70.1
SR04-36	268	12142	1.2	2.31229	2.8	0.20479	1.2	0.43	1201.0	13.5	1216.1	20.2	**1242.9**	50.4
SR04-37	125	2477	3.1	0.60291	5.3	0.07054	2.2	0.42	**439.4**	9.5	479.1	20.3	673.6	102.8
SR04-38	186	13298	2.7	2.97523	2.0	0.23731	1.2	0.61	1372.7	15.3	1401.3	15.4	**1445.1**	30.5
SR04-39	639	34922	23.0	1.69735	2.7	0.16870	1.7	0.63	1005.0	15.9	1007.5	17.2	**1013.1**	42.2
SR04-40	371	18326	0.8	2.27699	2.2	0.20061	1.5	0.71	1178.6	16.6	1205.2	15.2	**1253.1**	29.6
SR04-41	36	2086	1.2	1.61695	5.3	0.16426	1.8	0.34	980.4	16.7	976.8	33.6	**968.7**	102.5
SR04-42	139	4315	1.1	0.96903	4.0	0.11012	3.4	0.87	**673.4**	22.0	688.0	19.8	735.7	41.8
SR04-43	273	18105	1.9	3.82241	4.4	0.27798	4.1	0.93	1581.2	57.8	1597.5	35.8	**1619.0**	31.0
SR04-44	289	5246	2.1	0.46193	4.7	0.06036	2.7	0.57	**377.8**	9.8	385.6	15.1	432.5	86.2
SR04-45	90	2637	1.1	0.75874	3.7	0.08994	2.4	0.63	**555.2**	12.5	573.3	16.4	645.8	62.4
SR04-46	210	20972	2.9	4.21090	6.3	0.29767	5.8	0.91	1679.8	85.8	1676.1	52.1	**1671.6**	47.5
SR04-47	536	17308	3.9	0.85338	3.9	0.10269	3.1	0.78	**630.2**	18.4	626.5	18.3	613.2	52.6
SR04-48	345	40453	1.2	11.59918	5.9	0.49147	5.5	0.92	2577.0	115.8	2572.6	55.3	**2569.1**	38.1
SR04-48A	174	10843	1.5	4.84378	4.7	0.31659	3.1	0.65	1773.0	47.7	1792.5	39.8	**1815.3**	65.2
SR04-49	98	7142	2.5	2.25183	2.3	0.20275	1.0	0.44	1190.1	10.9	1197.4	16.0	**1210.5**	40.3
SR04-50	25	1829	1.5	2.36761	3.3	0.20880	1.3	0.39	1222.4	14.2	1232.9	23.5	**1251.2**	59.6
SR04-51	24	1544	2.5	1.84727	4.7	0.17038	3.8	0.82	1014.2	36.0	1062.5	30.7	**1162.9**	52.7
SR04-52	550	6190	0.8	0.42098	10.0	0.05471	7.3	0.71	**343.4**	24.4	356.8	30.9	444.8	160.9
SR04-52A	440	9711	1.7	0.60473	1.8	0.07391	1.4	0.76	**459.6**	6.1	480.2	6.9	579.7	25.6
SR04-55	361	6123	0.3	0.82914	2.2	0.09774	1.5	0.67	**601.2**	8.6	613.1	10.2	657.6	35.0
SR04-53	201	13203	2.0	2.34469	2.0	0.20856	1.7	0.87	1221.1	19.3	1225.9	14.3	**1234.4**	19.7

Table 2 (Continued). LA-MC-ICPMS U-Th-Pb data of detrital zircons from silty sandstone SR04, Lower Santa Rosa Formation, La Concordia, Chiapas. (Long. 92.6075º W, Lat. 15.9890º N.

Grain-spot	U ppm	$^{206}Pb/^{204}Pb_c$	$^{232}Th/^{238}U$	$^{207}Pb^*/^{235}U$ ± 1σ %		$^{206}Pb^*/^{238}U$ ± 1σ %		Err corr	Apparent ages $^{206}Pb/^{238}U$ (Ma) ±1σ		$^{207}Pb/^{235}U$ (Ma) ±1σ		$^{207}Pb/^{206}Pb$ (Ma) ±1σ	
(1)				(2)		(2)			(3)				(3)	
SR04-54	74	3614	1.0	2.24511	2.9	0.19414	1.9	0.67	1143.8	20.2	1195.3	20.2	**1289.5**	41.5
SR04-56	430	19160	1.0	1.48718	2.9	0.15380	2.3	0.80	922.2	20.1	925.2	17.7	**932.1**	35.7
SR04-57	129	6997	2.5	1.67458	3.0	0.16649	2.3	0.76	992.7	20.7	998.9	18.9	**1012.5**	39.1
SR04-58	620	38677	1.7	2.25829	2.3	0.20382	1.3	0.56	1195.8	14.4	1199.4	16.4	**1205.7**	38.0
SR04-59	29	1541	1.7	1.74324	3.8	0.17309	2.1	0.55	1029.1	20.1	1024.7	24.6	**1015.1**	64.4
SR04-60	218	20712	2.0	7.50146	4.0	0.40076	3.5	0.88	2172.6	65.5	2173.2	36.3	**2173.7**	33.8
SR04-61	100	9153	1.9	4.04604	3.4	0.29239	1.8	0.54	1653.5	26.7	1643.5	27.3	**1630.8**	52.3
SR04-62	172	5376	1.2	0.97310	4.3	0.11265	2.5	0.58	**688.1**	16.3	690.1	21.7	696.4	75.5
SR04-63	37	831	0.7	0.47620	8.6	0.06231	5.8	0.67	**389.7**	21.8	395.5	28.1	429.5	141.3
SR04-64	222	9910	4.2	1.33160	5.1	0.14175	3.1	0.61	**854.6**	25.0	859.6	29.6	872.5	83.7
SR04-64A	272	9170	1.3	0.96871	3.8	0.11077	3.6	0.95	**677.2**	23.4	687.8	19.0	722.6	24.3
SR04-65	330	9259	1.4	0.73009	4.3	0.08930	4.1	0.94	**551.4**	21.6	556.6	18.6	578.0	32.0
SR04-66	378	26308	8.7	3.26711	2.2	0.25591	1.9	0.84	1468.9	24.7	1473.3	17.4	**1479.5**	23.1
SR04-67	125	3228	0.7	0.73117	3.6	0.08917	2.8	0.80	**550.6**	15.0	557.2	15.3	584.4	46.6
SR04-68	282	8068	1.6	0.95323	3.8	0.10873	3.3	0.88	**665.4**	21.1	679.8	18.7	727.8	37.4
SR04-69	95	9359	0.7	5.83302	4.1	0.35609	3.7	0.90	1963.6	62.5	1951.3	35.6	**1938.3**	31.9
SR04-70	517	31271	5.9	3.40704	6.9	0.25839	5.5	0.81	1481.6	73.1	1506.0	53.8	**1540.6**	76.4
SR04-70A	154	11242	1.5	2.83578	2.9	0.23479	2.5	0.87	1359.5	30.8	1365.1	21.8	**1373.7**	27.8
SR04-71	181	9081	1.6	2.37467	4.0	0.21175	3.8	0.96	1238.2	43.1	1235.0	28.4	**1229.5**	21.5
SR04-72	172	16773	1.7	7.67171	4.7	0.40191	4.3	0.91	2177.8	79.5	2193.3	42.4	**2207.8**	33.5
SR04-73	430	5602	0.6	0.39242	4.1	0.05268	3.1	0.76	**330.9**	9.9	336.1	11.6	372.3	59.8
SR04-74	101	5466	2.0	1.89810	3.7	0.18256	3.5	0.95	1080.9	34.7	1080.4	24.4	**1079.4**	23.2
SR04-75	302	42913	1.4	23.51224	3.5	0.62184	2.4	0.68	3117.2	59.1	3248.4	34.5	**3330.4**	40.9
SR04-76	73	1259	0.5	0.40106	9.8	0.05345	4.9	0.50	**335.6**	15.9	342.4	28.5	388.6	191.2
SR04-76A	153	16753	1.7	7.27933	4.2	0.39736	3.8	0.90	2156.9	69.5	2146.3	37.9	**2136.2**	33.1
SR04-77	27	1033	2.3	1.11226	6.2	0.11282	2.5	0.40	**689.1**	16.2	759.3	33.1	971.8	115.6
SR04-78	47	1194	1.2	0.90127	6.1	0.10702	3.6	0.59	**655.4**	22.4	652.4	29.3	641.9	105.6
SR04-79	1177	13722	6.6	0.43941	3.4	0.05928	3.2	0.95	**371.3**	11.5	369.8	10.4	360.9	23.4
SR04-80	141	7848	2.3	2.33860	3.1	0.20801	2.2	0.71	1218.2	24.1	1224.1	21.8	**1234.4**	42.3
SR04-81	182	3591	2.5	0.55303	2.8	0.06900	2.1	0.77	**430.1**	8.8	447.0	10.0	534.7	38.8
SR04-82	85	3721	1.7	1.78182	3.3	0.17594	2.5	0.76	1044.8	24.4	1038.8	21.5	**1026.4**	43.2
SR04-83	112	2553	1.7	1.03973	2.8	0.11745	2.4	0.86	**715.9**	16.6	723.8	14.7	748.4	30.3
SR04-84	61	6341	0.9	7.20882	3.6	0.39309	3.1	0.88	2137.1	56.9	2137.6	31.7	**2138.0**	29.6
SR04-85	75	7847	4.0	7.02709	5.1	0.38895	1.2	0.23	2117.9	21.0	2114.9	45.7	**2111.9**	87.8
SR04-86	227	17401	2.4	3.95388	3.3	0.28674	2.5	0.76	1625.2	35.7	1624.8	26.5	**1624.2**	39.5
SR04-87	194	4810	1.7	0.81375	6.0	0.09440	4.7	0.78	**581.5**	26.0	604.6	27.4	691.9	80.2
SR04-87A	312	7516	7.7	0.74880	3.5	0.09075	2.4	0.68	**560.0**	12.8	567.5	15.3	598.0	56.3
SR04-88	107	2196	0.7	0.65247	4.2	0.08122	3.9	0.94	**503.4**	19.0	510.0	16.7	539.6	30.0
SR04-88A	93	2486	2.5	0.71446	4.5	0.08647	3.5	0.79	**534.6**	18.0	547.4	18.9	600.8	59.6
SR04-89	174	2187	0.7	0.40247	5.3	0.05427	4.2	0.80	**340.7**	14.1	343.4	15.4	362.3	71.0
SR04-90	87	1725	2.5	2.49384	6.6	0.21839	2.0	0.30	1273.3	22.7	1270.2	48.0	**1265.0**	123.6
SR04-91	1916	21069	60.3	0.45322	4.8	0.06204	2.3	0.48	**388.0**	8.7	379.5	15.1	328.1	95.1
SR04-94	215	9526	3.7	2.18891	4.7	0.19922	3.5	0.74	1171.1	37.2	1177.5	32.5	**1189.3**	61.4
SR04-95	211	2765	1.6	0.47406	5.4	0.06057	2.9	0.54	**379.1**	10.9	394.0	17.7	482.5	100.8
SR04-96	159	3831	0.7	0.79844	3.4	0.09721	1.9	0.57	**598.0**	11.0	596.0	15.3	588.1	60.7
SR04-97	383	24425	2.4	4.07071	3.3	0.29356	2.9	0.89	1659.3	43.0	1648.5	26.8	**1634.6**	27.3
SR04-98	693	6558	2.4	0.74386	8.5	0.08731	2.4	0.28	**539.6**	12.4	564.7	36.8	666.8	174.7
SR04-99	149	14114	2.1	8.04827	3.9	0.41590	3.8	0.96	2241.8	71.0	2236.5	35.4	**2231.5**	19.5
SR04-100	149	8119	2.2	2.21892	3.0	0.20235	2.4	0.79	1187.9	25.9	1187.0	21.1	**1185.3**	36.5

(1) Sample identifier–spot number; (2) Isotope ratios corrected for common Pb using measured ^{204}Pb for correction. Individual errors are given as 1 sigma standard deviation; (3) Most reliable apparent ages are indicated in **bold**. Note: If the average of apparent ages is mid-Proterozoic and older (>900 Ma) then $^{207}Pb/^{206}Pb$ ages are considered as most reliable apparent ages; for younger values $^{206}Pb/^{238}U$ ages are used.

the youngest detrital grains have an age peak at ~319 Ma. Sample SR04 does not contain any zircon of the latter age group. Provided that this is not simply a coincidence, the depositional age at outcrop SR04 can be bracketed between ~335 and ~319 Ma in the Late Mississippian to Early Pennsylvanian, which is consistent with the age of crinoids described from the sequence (Hernández-García, 1973).

The sediments at outcrop SR03 that are stratigraphically ~3000 meters higher must be younger than 319 Ma. If the arguments from the paleontological record are true, the

Upper SRF starts with beds of Desmoinesian (Hernández-García, 1973) age which is part of the Moscovian (Middle Pennsylvanian) stage that spans from ~312 to ~307 Ma (Heckel and Clayton, 2006). This restricts the depositional age at outcrop SR03 within a relatively short time interval after 319 Ma in the latest Early Pennsylvanian. It also suggests that SR03 must be relatively close to the upper limit (within the first kilometer) of the Lower SRF.

On the basis of these considerations, we can assume that ~3000 meters of monotonous clastic sediments between samples SR03 and SR04 probably accumulated within an interval less than 15 Ma. If stratigraphic relations are correct then the sedimentation rate was 20 cm/ka or more. If the original thickness of the monotonous sequence is about 6300 meters as suggested by Hernandez-García (1973), then another 3000 meters may be flooded or buried below SR04. Assuming similar sedimentation rates, the stratigraphic base of the Lower SRF may be as old as 350–340 Ma. Admittedly, the number of assumptions makes this age estimate speculative but it is in good agreement with ~345 Ma old conodonts reported from shales and limestones close to Salamá, which cover a basal conglomerate above the San Gabriel Sequence of central Guatemala (Solari *et al.*, in press; Ortega-Obregón, 2005). The Guatemalan Mississippian shales and limestones were correlated with the Sacapulas Formation (Bohnenberger, 1966), which are the lowermost strata of the Santa Rosa Group in Guatemala (Figure 2). Thus, our data can be viewed as consistent with the idea that the Lower SRF in Chiapas and the lower strata from the Santa Rosa Group in Guatemala (namely Sacapulas, Salamá, Chicol) were deposited at about the same time in apparently different depositional environments. This is in contrast to Hernández-García (1973), who interpreted the Lower SRF as an independent, discordant sequence which is older and not correlative with the Santa Rosa Group. Besides that, a 10 m thick conglomerate described by Hernández-García (1973) in the Lower SRF may be related to a basal conglomerate that characterizes the base of the Santa Rosa Group in Guatemala (Chicol Formation, Clemons and Burkart, 1971).

Provenance

Probability plots of the age results from both samples of the Lower SRF (Figures 7a, 7b) are shown together with age probability distributions of the Upper SRF (Figures 7c, 7d; Weber *et al.*, 2006), the Santa Rosa Group equivalent Macal Series of Belize (Figure 7e; Martens *et al.*, submitted), the Paleozoic Cosoltepec Formation of the Acatlán Complex (Figures 7f-7h; Talavera-Mendoza, *et al.*, 2005; Keppie *et al.*, 2006), and Mississippian to Pennsylvanian strata that cover the Oaxacan Complex (Figures 7i, 7j; Gillis *et al.*, 2005).

The age distributions of zircons from the Lower SRF are similar to those from the Upper SRF close to the village of Chicomuselo (Weber *et al.*, 2006). Most of the zircons from the Lower SRF have ages within the time span of the Pan-African-Brasiliano orogenic cycle in the Neoproterozoic, which clearly indicate Gondwana provenance for the sediments. Moreover, the zircons in the range from 700 to 500 Ma of both samples have probablility peaks at about 550 as well as around 620 Ma, which is also consistent with the ages of most Pan-African-Brasiliano zircons dated from the Upper SRF (Weber *et al.*, 2006).

In the stratigraphically lower sample SR04, another important group of zircons have Mesoproterozoic ages (1.6–0.9 Ga), whereas SR03 lacks a significant peak of this age (Figures 7a, 7b). The most prominent Mesoproterozic ages are the range from 1.3 to 1.2 Ga, whereas typical Grenville-age (1.0 Ga) zircons are less abundant. Zircons from the Mesoproterozoic basement outcrops of the Oaxacan and Guichicovi complexes record both 1.0 and 1.3–1.2 Ga events (Weber and Köhler, 1999; Solari *et al.*, 2003), but zircons formed during the 1.0 Ga orogeny, which is by far the most important event, dominate in the sediments shed from the Oaxacan complex (Figures 7i, 7j; Gillis *et al.*, 2005). The presence of 1.2–1.0 Ga zircons further suggests that the sediment was derived partially from South America rather than from Africa because the West African craton was not involved in the Grenville orogeny (*e.g.*, Dalziel, 1997). In present-day Brazil and Bolivia, the Grenville orogeny is represented by the 0.9–1.1 Ga Sunsás province. Sunsás is stitched together with the 1.25–1.4 Ga Rondônia-San Ignacio Igneous Province that includes also a 1.2 Ga orogeny (Tohver *et al.*, 2002, 2004), and the 1.5–1.8 Ga Rio Negro-Juruena Province (Tassinari *et al.*, 2000). Detrital zircons with ages that coincide with the age of either of these South American provinces occur in the lower SRF samples. The age distribution of Mesoproterozoic zircons together with the presence of Trans Amazonian-age (1.9–2.2 Ga) zircons, indicate a provenance of these sediments from southwestern Gondwana.

Silurian to Devonian igneous rocks, which are represented by several detrital grains, are common in the Maya Mountains of Belize (Steiner and Walker, 1996), in Guatemala (Solari *et al.*, in press; Ortega-Obregon, 2005), and were recently also recognized in the Motozintla area of Chiapas (Salazar-Juárez *et al.*, 2007). It is noteworthy, however, that Silurian to Devonian zircons are relatively rare in the SRF compared to zircons from Pan-African-Brasiliano rocks, which are not exposed in the Maya block or adjacent terranes. On the other hand, flysch-type sediments of the Macal formation from the Maya Mountains in Belize that were correlated with the Santa Rosa Group (Bateson and Hall, 1977) contain almost exclusively zircons from surrounding Silurian to Devonian igneous rock (Figure 7e; Martens *et al.*, submitted).

The similarity of provenance ages from both the Upper and the Lower SRF indicates that sediment source regions and transport mechanisms did not change significantly between the Upper and the Lower SRF. Thus, the expected

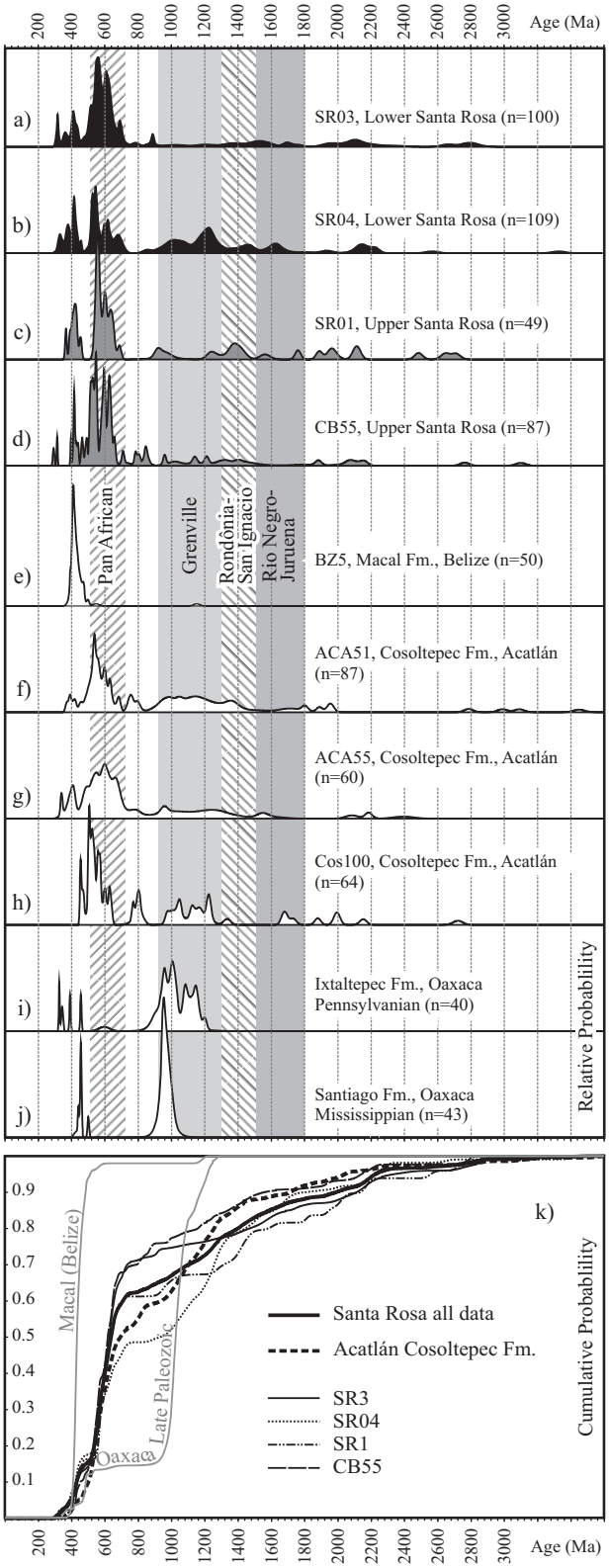

stratigraphic discontinuity between the deposition of the Upper and the Lower SRF as suggested by Hernández-García (1973) in not recorded by the age patterns. An angular unconformity between the two, as observed by Hernández (1973), could be a local phenomena like a refilled submarine channel or a sequence-stratigraphic boundary within the same flysch-type sequence, which might be continuous from the Mississippian to the Upper Pennsylvanian similar as suggested for the Santa Rosa Group in Guatemala (Clemons and Burkart, 1971). However, there is an apparent difference in the contribution of Mesoproterozoic zircons between the straigraphically lower sample SR04 (Figure 7b) and the other samples analyzed form the SRF (Figures 7a, 7c, 7d).

Regional tectonic and stratigraphic implications

Collision of Gondwana with Laurentia and diachronous closure of the Rheic Ocean led to the Alleghenian orogeny (*e.g.*, Murphy *et al.*, 2006). This orogeny lasted from ~320 to ~280 Ma, starting in the northern Appalachians and ending in the Marathon-Ouachita belt (*e.g.*, Hatcher, 2002). The overwhelming abundance of zircons from Pan-African-Brasialiano belts was attributed to erosion of these newly formed Alleghenian mountain ranges and deposition of flysch-type sediments onto the Maya block (Weber *et al.*, 2006). However, accepting the work of Murphy *et al.* (2006), in the Late Mississippian (~340–320 Ma) western Gondwana was approaching to Laurentia by closure of the Rheic ocean (*e.g.*, Keppie, 2004 and references therein). During this time, the fraction of Mesoproterozoic sources in the transportation currents draining to the passive margin of NW Gondwana may still have been of greater importance with respect to the input from Pan-African-Brasiliano belts as suggested by the abundance of Mesoproterozoic zircons in sample SR04 of probably Late Mississippian depositional age (see above).

Comparison of the detrital zircon age data for the SRF with published data for other Paleozoic sedimentary rocks and protoliths of southern Mexico (Figure 7), reveals an outstanding similarity between provenance age patterns of the SRF and the Cosoltepec Formation of the Acatlán Complex in the Mixteca terrane (Figures 1, 2, 7f-7h; Talavera-Mendoza *et al.*, 2005; Keppie *et al.*, 2006). As shown in Figure 7k, the cumulative probalility curve of all data from the Cosoltepec Formation is fairly congruent with

Figure 7. a-j: Age probablility plots of detrital zircons from (a, b) the Lower Santa Rosa Formation (this work), (c, d) the Upper Santa Rosa Formation (Weber *et al.*, 2006), (e) the Macal Formation from the Maya Mountains, Belize (Martens *et al.*, submitted), (f-h) the Cosoltepec Formation from the Acatlán complex in the Mixteca terrane (f, g: Talavera-Mendoza *et al.*, 2005; h: Keppie *et al.*, 2006), (i, j) from Carboniferous strata covering the Oaxacan complex in the Zapoteco terrane (Gillis *et al.*, 2005). k: Cumulative probability curves for detrital zircon ages of individual samples from the Santa Rosa Formation together with the cumulative probability curve of all Santa Rosa data. Note that the cumulative probability curve of the data from the Cosoltepec Formation is similar to that of the Santa Rosa Formation and particularly to SR04. Grey probability curves calculated from the Belize and from the Oaxaca data instead, are different.

the probalility curves for the SRF data. This is especially true for the probability curve of SR04 in which Mesoproterozoic zircons are more abundant.

However, the Cosoltepec Formation (and the Acatlán Complex) has never been correlated with the SRF. On the basis of detrital zircon ages and field relationships the maximum depositional age of the Cosoltepec Formation was estimated to be Devonian (Talavera-Mendoza *et al.*, 2005) or Ordovician to Mississippian (Keppie *et al.*, 2006). However, Talavera-Mendoza *et al.* (2005) reported one detrital grain of 341 ± 7 Ma that was considered (correctly) not to be reliable and Keppie *et al.* (2006) argued that the Cosoltepec Formation must be older than ~305 Ma old overlying sediments (Tecomate Formation, Figure 2). On the basis of these arguments, Late Mississippian to Middle Pennsylvanian can be a plausible time interval for the deposition of the Cosoltepec Formation. By assuming such a depositional age, the comparable distributions of zircon ages (Figure 7) suggest that at least part of the sediments constituting the Cosoltepec Formation may correlate with beds from SRF. The scope of this contribution is not adequate to proof this hypothesis, but the possibility of Carboniferous correlations across southern Mexico should be considered in future works.

Within the Zapoteco terrane, detrital zircon ages of Paleozoic sedimentary rocks that cover the Proterozoic Oaxacan complex (Figures 1, 2) differ from those of the SRF (Figures 7i, 7j; Gillis *et al.*, 2005). Both, Pennsylvanian Ixtaltepec Formation and Mississippian Santiago Formation have mainly Mesoproterozoic detrital zircons and the spectra contain no ages of Pan-African-Brasiliano or of Paleoproterozoic-Archaean provenance. The Mesoproterozoic basement of the Oaxacan complex is commonly correlated with some basement outcrops of the Chortis block (Manton, 1996; Nelson *et al.*, 1997). If this correlation is correct then sedimentary rocks from the Chortis block should have detrital zircon ages similar to those of the Zapoteco terrane. Thus, detrital zircon ages may also distinguish sedimentary rocks of the Chortis block from those of the Santa Rosa Group, which in turn can help to define the limit between the Chortis and the Maya blocks.

Silurian-Devonian and older sedimentary rocks were recently reported from different locations in the southern Maya block, including Maya Mountains (Martens *et al.*, 2006 and submitted), central Guatemala (Ortega-Obregón, 2005; Solari *et al.*, in press), and the Chiapas Massif (Pompa-Mera *et al.*, 2007). Our results indicate that early Paleozoic sediments are not part of the SRF. The entire Santa Rosa Group is probably younger than Devonian and covers an older sequence with detritus that comes from different, mainly Mesoproterozoic sources (Martens *et al.*, 2006 and submitted; Weber *et al.*, 2007, 2008). The subdivision into Upper and Lower SRF is not recorded by the detrital zircon age spectra and might be avoided. As a simplification, we suggest the usage of the term Santa Rosa Group, like in Guatemala, also for the Carboniferous-Permian strata in Chiapas. However, the Santa Rosa Group (Carboniferous-Permian) may be underlain by Lower Devonian or older strata. It will be a future challenge to identify and correlate Paleozoic strata occurring in the Maya block and adjacent crustal blocks, including the Maya-Chortis border zone.

ACKNOWLEDGEMENTS

This work was supported by CONACYT project D41083-F. Many thanks to Susana Rosas-Montoya and Víctor Pérez-Arroyoz (CICESE) for their help with preparing the zircon separates and thin sections. Arizona LaserChron Center is partially supported by NSF Instrumentation and Facilities Program grant (NSF-EAR 0443387). We are grateful to Thomas H. Anderson, Univerity of Pittsburgh, and Brent V. Miller, Texas A&M University, for their helpful and comprehensive reviews.

REFERENCES

Anderson, T.H., Schmidt, V.A., 1983, The evolution of Middle America and the Gulf of Mexico – Caribbean Sea region during Mesozoic time: Geological Society of America, 94(8), 941-966.

Anderson, T.H., Erdlac, R.J., Jr., Sandstrom, M.A., 1985, Late-Cretaceous allochthons and post-Cretaceous strike-slip displacement along the Cuilco-Chixoy-Polochic Fault, Guatemala: Tectonics, 4(5), 453-475.

Bateson, J.H., Hall, I.H.S., 1977, The geology of the Maya Mountains: Belize: Institute of Geological Science, Her Majesty´s Stationery Office, Overseas Memoir 3, 43 p.

Bohnenberger, O.H., 1966, Nomenclatura de las capas Santa Rosa en Guatemala: Guatemala, Publicaciones Gelógicas del Instituto Centroamericano de Investigación y Tecnología (ICAITI), 1, 47-51.

Burkart, B., Self, S., 1985, Extension and rotation of crustal blocks in northern Central America and effect on the volcanic arc: Geology, 13, 22-26.

Burkart, B., Deaton, B.C., Dengo, C., Moreno, G., 1987, Tectonic wedges and offset Laramide structures along the Polochic fault of Guatemala and Chiapas, Mexico: Reaffirmation of large Neogene displacements: Tectonics, 6, 411-422.

Clemons R.E., Burkart, B., 1971, Stratigraphy of Northwestern Guatemala: Boletín de la Sociedad Geológica Mexicana, 32(2), 143-158.

Dalziel, W.D.I., 1997, Neoproterozoic–Paleozoic geography and tectonics: review, hypothesis, environmental speculation: Bulletin of the Geological Society of America, 109(1), 16-42.

Damon, P.E., Shafiqullah, M., Clark, K., 1981, Age trends of igneous activity in relation to metallogenesis in the southern Cordillera, *in* Dickinson, W., Payne, W.D. (eds.), Relations of Tectonics to Ore Deposits in the Southern Cordillera: Tucson, Arizona, Arizona Geological Society Digest, 14, 137-153.

Dengo, G., 1985, Mid America: Tectonic setting for the Pacific margin from southern México to northwestern Colombia, *in* Nairn, A.E.M., Stehli, F.G. (eds.), The Oceanic Basins and Margins, 7a. The Pacific Ocean: New York, Plenum Press, 123-180.

Dickinson, W.R., Gehrels, G.E., 2003, U–Pb ages of detrital zircons from Permian and Jurassic eolian sandstones of the Colorado Plateau, USA: paleogeographic implications: Sedimentary Geology, 163, 29-66.

Dixon, C.G., 1956, Geology of southern British Honduras with notes on adjacent areas: Belize, Government Printer, Survey Department, 85 p.

Estrada-Carmona, J., Weber, B., Hecht, L., Martens, U., 2009, P-T-t tra-

jectory of metamorphic rocks from the central Chiapas Massif Complex: the Custepec unit, Chiapas, Mexico: Revista Mexicana de Ciencias Geológicas, 26(1), 243-259.

Fedo, C.M., Sircombe, K.N., Rainbird, R.H., 2003, Detrital zircon analysis of the sedimentary record, *in* Hanchar, J.M., Hoskin, P.W.O. (eds.), Zircon: Reviews in Mineralogy and Geochemistry, 53, 277-303.

French, C.D., Schenk, C.J., 1997, Map showing geology, oil and gas fields, and geologic provinces of the Caribbean region: United States Geological Survey, Open File Report 97-470-K.

Gehrels, G., Valencia, V., Pullen, A., 2006, Detrital zircon geochronology by Laser-Ablation Multicollector ICPMS at the Arizona LaserChron Center, *in* Olszewski, T., (ed.), Geochronology: Emerging Opportunities, Paleontological Society Short Course: Philadelphia, PA, Paleontological Society Papers, 12, 67-76.

Gehrels, G.E., Valencia, V.A., Ruiz, J., 2008, Enhanced precision, accuracy and efficiency, and spatial resolution of U-Pb ages by LA-MC-ICPMS: Geochemistry Geophysics Geosystems, 9, Q03017, doi: 10.1029/2007GC001805.

Gillis, R.J., Gehrels, G.E., Ruiz, J, Flores de Dios González, L.A., 2005, Detrital zircons provenance of Cambrian-Ordovician and Carboniferous strata of the Oaxaca terrane, southern Mexico: Sedimentary Geology, 182, 87-100.

Hatcher, R.D., 2002, Alleghanian (Appalachian) orogeny, a product of zipper tectonics: Rotational transpressive continent-continent collision and closing of ancient oceans along irregular margins, *in* Martínez-Catalán, J.R., Hatcher, R.D., Arenas, R., Díaz-García, F. (eds.), Variscan-Appalachian Dynamics: The building of the late Paleozoic basement: Boulder Colorado, Geological Society of America, Special Paper 364, 199-208.

Heckel, P., Clayton, G., 2006, The Carboniferous System. Use of the new official names for the subsystems, series and stages: Geologica Acta, 4 (3), 7-11.

Hernández-García, R., 1973, Paleogeografía del Paleozoico de Chiapas, México: Boletín de la Asociación Mexicana de Geólogos Petroleros, 25, 79-113.

Jiménez-Hernández, A., Jaimez-Fuentes, A., Motolinía-García, O., Pinzón-Salazar, T., Membrillo-Ortega, H., 2005, Carta Geológica-Minera Huixtla D15-2, escala 1:250,000: Pachuca, Hidalgo, México, Servicio Geológico Mexicano, 1 map.

Keppie, J.D., 2004, Terranes of Mexico revisited: A 1.3 billion year odyssey: International Geology Review, 46, 765-794.

Keppie, J.D., Nance, R.D., Fernández-Suárez, J., Storey, C.D., Jeffries, T.E., Murphy, J.B., 2006, Detrital zircon data from the eastern Mixteca terrane, southern Mexico: evidence for an Ordovician–Mississippian continental rise and a Permo-Triassic clastic wedge adjacent to Oaxaquia: International Geology Review, 48, 97-111.

López-Ramos, E., 1979, Geología de México, Tomo III: México D.F., Edición privada, 446 p.

Ludwig, K.R., 2003, ISOPLOT: A geochronological toolkit for Microsoft Excel, Version 3.00: Berkeley Geochronology Center, Special publication 4, 70 p.

Manton, W.I., 1996, The Grenville of Honduras (abstract), *in* Geological Society of America, Annual meeting: Denver, CO, Geological Society of America, Abstracts with Programs, 28, A-493.

Martens, U., Weber, B., Valencia, V., 2006, Zircon geochronology implies the existence of pre-Devonian sedimentary rocks with Grenvillian provenance in the Maya Mountains of Belize (abstract), *in* Geological Society of America, Annual meeting: Denver, CO, Geological Society of America, Abstracts with Programs, 38(7), 504.

Martens, U., Weber, B., Valencia, V.A., submitted, U/Pb geochronology proves the existence of lower Paleozoic beds in the Maya block of Central America, and its affinity with Avalonian-type peri-Gondwanan terranes: Geological Society of America Bulletin.

Martínez-Amador, H., Rosendo-Brito, B., Fitz-Bravo, C., Tinajera-Fuentes, E., Beltrán-Castillo, H.D., 2005, Carta Geológica-Minera Tuxtla Gutiérrez E5-11, escala 1:250,000: Pachuca, Hidalgo, México, Servicio Geológico Mexicano, 1 map.

Murillo-Muñeton, G., 1994, Petrologic and geochronologic study of Grenville-age granulites and post-granulite plutons from the La Mixtequita area, state of Oaxaca in southern México, and their tectonic significance: Los Angeles, University of Southern California, M.S. thesis,163 p.

Murphy, J.B., Gutiérrez-Alonso, G., Nance, D.R, Fernández-Suárez, J., Keppie, J.D., Quesada, C., Strachan, R.A., Dostal, J., 2006, Origin of the Rheic Ocean: Rifting along a Neoproterozoic suture: Geology, 34, 325-328.

Nelson, B.K., Herrmann, U.R., Gordon, M.B., Ratschbacher, L., 1997, Sm-Nd and U-Pb evidence for Proterozoic crust for in the Chortís block, Central America: Comparison with the crustal history of southern Mexico (abstract): Terra Nova, 9, Abstract Supplement 1, p. 496.

Ortega-Gutiérrez, F., Mitre-Salazar, L.M., Roldán-Quintana, J., Aranda-Gómez, J.J., Morán-Zenteno, D., Alaniz-Álvarez, S.A., Nieto-Samaniego, A.N., 1992, Carta geológica de la República Mexicana, escala 1:2,000,000: México, Universidad Nacional Autónoma de México, Instituto de Geología.

Ortega-Gutiérrez, F., Solari, L.A., Ortega-Obregón, C., Elías-Herrera, M., Martens, U., Morán-Icál, S., Chiquín, M., Keppie, J.D., Torres de León, R., Schaaf, P., 2007, The Maya-Chortis boundary: a tectonostratigraphic approach: International Geology Review, 49(11), 996-1024.

Ortega-Obregón, C., 2005, Caracterización estructural petrológica y geoquímica de la zona de cizalla "Baja Verapaz", Guatemala: México, Universidad Nacional. Autónoma de México, M.S. thesis, 99 p.

Pompa-Mera, V., Solís-Pichardo, G., Schaaf, P., Weber, B., Hernández-Treviño, 2007. Geoquímica y geocronología de algunas rocas plutónicas del sector oriental del Macizo de Chiapas, México (resumen), *in* Reunión Anual de la Union Geofísica Mexicana, Puerto Vallarta, Jal., México: Geos, 27(1), p. 88.

Ruiz, J., Tosdal, R. M., Restrepo, P. A., Murillo-Muñeton, G., 1999, Pb isotope evidence for Colombia-southern Mexico connections in the Proterozoic, *in* Ramos, V. A., Keppie, J. D., (eds.), Laurentia-Gondwana connections before Pangea: Geological Society of America, Special Paper 336, 183–198.

Salazar-Juárez, J., Schaaf, P., Solís-Pichardo, G., Ortega-Gutiérrez, F., Elías-Herrera, M., Weber, B., 2007, Geología, petrología y geoquímica del Macizo de Chiapas, área de Motozintla de Mendoza (resumen), *in* Reunión Anual de la Union Geofísica Mexicana, Puerto Vallarta, Jal., México: Geos, 27(1), 87-88.

Sapper, K., 1899, Über Gebirgsbau und Boden des nördlichen Mittelamerika: Petermanns Geographische Mitteilungen, 27(127), 119 p.

Schaaf, P., Weber, B., Weis, P., Groß, A., Ortega-Gutiérrez, F., Köhler, H., 2002, The Chiapas Massif (México) revised: New geologic and isotopic data for basement characteristics, *in* Miller, H. (ed.), Contributions to Latin-American Geology: Neues Jahrbuch für Geologie und Paläontologie, Abhandlungen, 225, 1-23.

Solari, L. A., Keppie, J. D., Ortega-Gutiérrez, F., Cameron, K. L., Lopez, R., Hames, W. E., 2003, 990 and 1100 Ma Grenvillian tectonothermal events in the northern Oaxacan complex, southern México: roots of an orogen: Tectonophysics, 365, 257-282.

Solari, L.A., Ortega-Gutiérrez, F., Elías-Herrera, M., Schaaf, P., Norman, M., Torres de León, R., Ortega-Obregón, C., Chiquín, M., Morán-Ical, S., in press, U-Pb zircon geochronology of Paleozoic units in Western and Central Guatemala: insights into the tectonic evolution of Middle America, *in* Pindell, J., James, K.H. (ed.), Origin of the Caribbean Plate: Journal of the Geological Society of London, Special Publication.

Stacey, J.S.K., Kramers, J.D., 1975, Approximation of terrestrial lead isotope evolution by a two-stage model: Earth and Planetary Science Letters, 26 (2), 207-221.

Steiner, M.B., Walker, J.D., 1996, Late Silurian Plutons in Yucatan: Journal of Geophysical Research, 101, 17727-17735.

Talavera-Mendoza, O., Ruiz, J., Gehrels, G.E., Meza-Figueroa, D.M., Vega-Granillo, R., Campa-Uranga, M.F., 2005, U–Pb geochronology of the Acatlán Complex and implications for the Paleozoic paleogeography and tectonic evolution of southern Mexico: Earth and Planetary Science Letters, 225, 682-699.

Tassinari, C.C.G., Bettencourt, J.S., Geraldes, M.C., Macambira, M.J.B., Lafon, J.M., 2000, The Amazonian Craton, *in* Cordani, U.G., Milani, E.J., Filho, A.T., Campos, D. A. (eds.), Tectonic Evolution of South America: Rio de Janeiro, Proceedings of the 31st International Geological Congress, 41-95.

Tohver, E., van der Pluijm, B.A., Van der Voo, R., Rizzotto, G., Scandolaria, J.E., 2002, Paleogeography of the Amazonian craton at 1.2 Ga: early Grenvillian collision with the Llano segment of Laurentia: Earth and Planetary Science Letters, 199, 185-200.

Tohver, E., van der Pluijm, B., Mezger, K., Essene, E., Scandolara, J., Rizzotto, G., 2004, Terrane transfer during the Grenville orogeny: tracing the Amazonian ancestry of southern Appalachian basement through Pb and Nd isotopes: Earth and Planetary Science Letters, 228, 161-176.

Weber, B., 1998, Die magmatische und metamorphe Entwicklung eines kontinentalen Krustensegments: Isotopengeochemische und geochronologische Untersuchungen am Mixtequita-Komplex, Südostmexiko: Münchner Geologische Hefte, A24, 176 p.

Weber, B., Köhler, H., 1999, Sm-Nd, Rb-Sr and U-Pb isotope geochronology of a Grenville terrane in Southern Mexico: Origin and geologic history of the Guichicovi complex: Precambrian Research, 96, 245-262.

Weber, B., Gruner, B., Hecht, L., Molina-Garza, R.S., Köhler, H., 2002, El descubrimiento de basamento metasedimentario en el macizo de Chiapas: la "Unidad La Sepultura": Geos, 22, 2-11.

Weber, B., Cameron, K.L., Osorio, M., Schaaf, P., 2005, A late Permian tectonothermal event in Grenville crust of the Southern Maya terrane: U-Pb zircon ages from the Chiapas massif, southeastern Mexico: International Geology Review, 47, 509-529.

Weber, B., Schaaf, P., Valencia, V., Iriondo, A., Ortega-Gutiérrez, F., 2006, Provenance ages of Late Paleozoic sandstones (Santa Rosa Formation) from the Maya block, SE Mexico – implications on the tectonic evolution of western Pangea: Revista Mexicana de Ciencias Geológicas, 23, 262-276.

Weber, B., Iriondo, A., Premo, W.R., Hecht, L., Schaaf, P., 2007, New insights into the history and origin of the southern Maya Block, SE México: U-Pb-SHRIMP zircon geochronology from metamorphic rocks of the Chiapas Massif: International Journal of Earth Sciences (Geologische Rundschau), 96, 253-269.

Weber, B., Valencia, V.A., Schaaf, P., Pompa-Mera, V., Ruiz, J., 2008, Significance of provenance ages from the Chiapas Massif complex (SE Mexico): Redefining the Paleozoic basement of the Maya block and its evolution in a peri-Gondwanan realm: Journal of Geology, 116, 619-639.

Manuscript received: December 16, 2007
Corrected manuscript received: March 24, 2008
Manuscript accepted: April 9, 2008